

Representational Stability of Truth in Large Language Models

Samantha Dies^{1‡}, Courtney Maynard¹, Germans Savcisens¹, and Tina Eliassi-Rad^{1,2,3}

¹Khoury College of Computer Sciences, Northeastern University, 440 Huntington Ave, #202, Boston, MA 02115 USA

²Network Science Institute, Northeastern University, 177 Huntington Ave, #1010, Boston, MA 02115 USA

³Santa Fe Institute, 1399 Hyde Park Road, Santa Fe, NM 87501 USA

‡dies.s@northeastern.edu

ABSTRACT

Large language models (LLMs) are widely used for factual tasks such as “What treats asthma?” or “What is the capital of Latvia?”. However, it remains unclear how stably LLMs encode distinctions between true, false, and neither-true-nor-false content in their internal probabilistic representations. We introduce *representational stability* as the robustness of an LLM’s veracity representations to perturbations in the operational definition of truth. We assess representational stability by (*i*) training a linear probe on an LLM’s activations to separate true from not-true statements and (*ii*) measuring how its learned decision boundary shifts under controlled label changes. Using activations from sixteen open-source models and three factual domains, we compare two types of neither statements. The first are fact-like assertions about entities we believe to be absent from any training data. We call these *unfamiliar* neither statements. The second are nonfactual claims drawn from well-known fictional contexts. We call these *familiar* neither statements. The unfamiliar statements induce the largest boundary shifts, producing up to 40% flipped truth judgments in fragile domains (such as word definitions), while familiar fictional statements remain more coherently clustered and yield smaller changes ($\leq 8.2\%$). These results suggest that **representational stability stems more from epistemic familiarity than from linguistic form**. More broadly, our approach provides a diagnostic for auditing and training LLMs to preserve coherent truth assignments under semantic uncertainty, rather than optimizing for output accuracy alone.

1 Introduction

Large language models (LLMs) are increasingly used as sources of information, yet their behavior often blurs the line between knowledge and plausibility [1, 2, 3]. People expect experts to distinguish between **True**, **False**, and **Neither** statements, yet it remains unclear whether LLMs form similarly structured internal representations. The stability of internal veracity representations in LLMs, i.e., how consistently they encode truth and falsity across related statements, is crucial for reliability and safety [4, 5, 6]. When this representational structure is unstable, LLMs often exhibit undesirable behaviors such as hallucinations [3, 7].

LLMs can appear factually competent even when their internal veracity representations are weakly separated or inconsistent. Such instability is one explanation for why small prompt or context changes can affect an LLM’s answers [6, 8, 9], with recent work suggesting that epistemic familiarity also shapes an LLM’s confidence and self-evaluation [10]. Prior work follows two paths: representation-based probing, which examines whether true and false statements form separable clusters in activation space [11, 12, 13], and in-context analyses, which test how output varies under persuasion [14, 15], phrasing [2, 16], or jailbreak attacks [17]. However, we lack a unified approach for identifying which kinds of statements disrupt an LLM’s latent factual representation [18].

We address this gap by analyzing *representational stability*: the consistency of an LLM’s veracity representations under controlled perturbations of a probe’s training data (see Figure 1). Inspired by Leitgeb’s notion of P -stability [19], a property of belief systems requiring stability under small evidential changes, we treat a statement’s embedding as a belief state and use representation-based probes to identify *truth directions*.

We analyze three factual domains, City Locations, Medical Indications, and Word Definitions, and five statement types (**True**, **False**, **Fictional**, **Synthetic**, and **Noise**). **Fictional** and **Synthetic** statements represent distinct **Neither** cases. **Fictional** statements originate from familiar imaginary worlds likely present in training corpora, whereas **Synthetic** statements are automatically generated to ensure unfamiliarity. We train a probe on activations from sixteen open-source LLMs to learn a baseline **True** vs. **Not True** direction. For our probe, we use **sAwMIL**: a max-margin, multiple-instance probe designed to incorporate **Neither** statements [12]. We then retrain the same probe under label perturbations (e.g., treating **Fictional** statements as **True**) to quantify shifts in inferred belief boundaries.

Across our experiments, LLMs maintain well-separated **True** and **False** representations, but both familiar and unfamiliar **Neither** statements occupy context-dependent regions. Unfamiliar **Synthetic** **Neither** statements induce the largest rotations and flip rates, showing

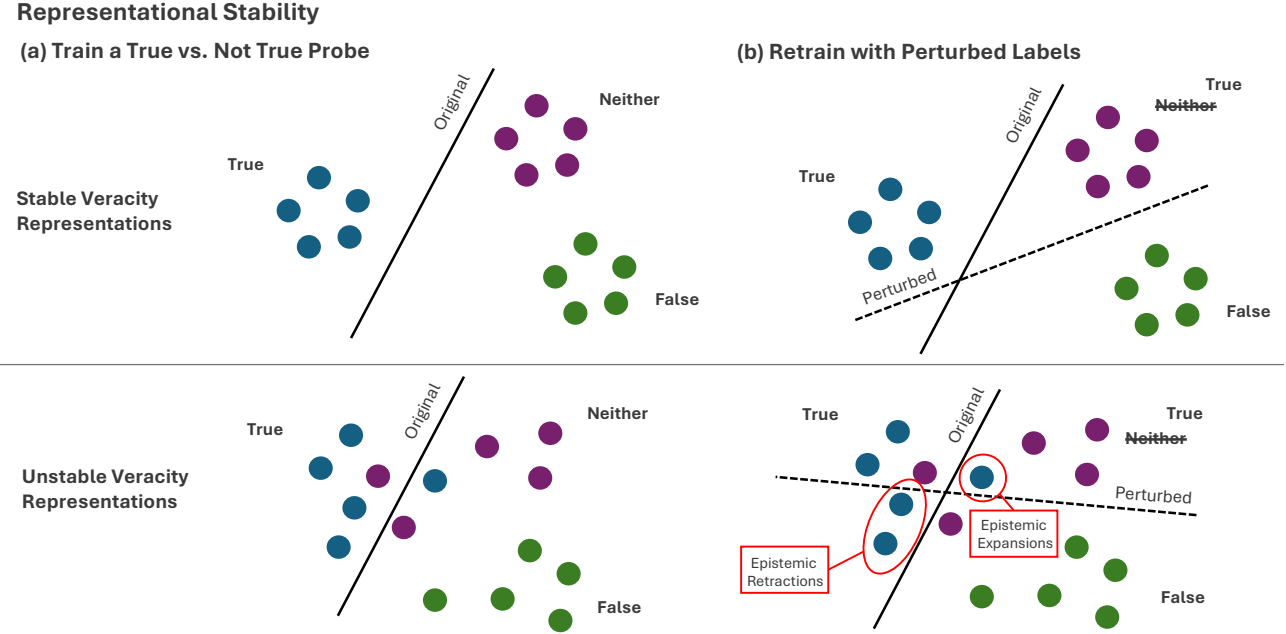


Figure 1. Overview of Representational Stability Evaluation. A toy example demonstrating how we assess representational stability by (a) training a True vs. Not True probe on LLM activations with True (blue), False (green) and Neither (purple) veracity values and (b) retraining the probe with perturbed labels (i.e., redefining the operational definition of truth to include the Neither statements). We compare the similarity between the original (solid) and perturbed (dashed) decision boundaries and identify how many True statements flip to Not True after the perturbation (epistemic retractions) or, conversely, how many Not True statements flip to True (epistemic expansions). Stable veracity representations should have well-clustered activations that minimize the number of epistemic retractions and expansions.

that unfamiliar content disrupts an LLM’s veracity structure more than familiar **Fictional** content. Together, these analyses provide a systematic and principled way to evaluate the robustness of LLM veracity representations under different semantic assumptions, an essential step toward diagnosing and mitigating factual inconsistency.

Contributions

- Data:** We introduce a new dataset of fictional statements across three factual domains, enabling controlled comparisons between familiar (**Fictional**) and unfamiliar (**Synthetic**) **Neither** content.
- Method:** We introduce and study *representational stability* in LLMs by combining activation-based probes with controlled label perturbations that vary the operational definition of truth.
- Representational Structure:** We show across sixteen open-source LLMs that True and False activations form tightly aligned clusters, while Neither statements (familiar and unfamiliar) occupy distinct regions, reflecting differences in training familiarity rather than superficial linguistic form.

4. **Stability:** We show that the unfamiliar **Synthetic** statements produce the largest rotations in the truth directions and the highest prediction flip rates (up to 40% in Word Definitions), indicating that previously unseen yet semantically factual content most strongly destabilizes veracity geometry.

2 Related Work

Understanding how LLMs encode veracity touches on three research threads: (1) representation-based probing, (2) in-context stability, and (3) epistemic distinctions between belief, knowledge, and fact. We connect these strands by examining how familiar and unfamiliar **Neither** statements perturb the latent veracity geometry, thereby assessing how stable an LLM’s representations are under shifts in semantic assumptions.

Representation-based probing methods determine which properties are linearly recoverable from hidden states, revealing what models represent beyond input-output behavior [20, 21, 22]. Much of this work focuses on linguistic or syntactic recoverability, but recent studies have examined geometric structure, specifically, whether True and False statements form separable or directionally aligned clusters in activation space [11, 13]. Of

Table 1. Summary of datasets and statement types. [†] Number of affirmative (A) and negated (N) statements for each type across the three datasets, along with examples. Each dataset includes **True**, **False**, **Synthetic**, and **Fictional** statements, while **Noise** consists of randomly generated Gaussian activation vectors matched in dimensionality and distribution to the real statement embeddings. **Synthetic** statements serve as **Neither** statements that were not seen during LLM training, while **Fictional** statements are familiar **Neither** statements.

Dataset	True	False	Synthetic	Fictional	Noise	Examples
City Locations	A: 1392 N: 1376	A: 1358 N: 1374	A: 876 N: 876	A: 350 N: 350	795	(T) The city of Surat is located in India. (Fa) The city of Palembang is located in the Dominican Republic. (S) The city of Norminsk is located in Jamoates. (Fi) The city of Bikini Bottom is located in the Pacific Ocean.
Medical Indications	A: 1439 N: 1522	A: 1523 N: 1419	A: 478 N: 522	A: 402 N: 402	771	(T) Pentobarbital is indicated for the treatment of insomnia. (Fa) Vancomycin is not indicated for the treatment of lower respiratory tract infections. (S) Alumil is indicated for the treatment of reticlers. (Fi) The Trump Virus is indicated for the treatment of Xenovirus Takis-B.
Word Definitions	A: 1234 N: 1235	A: 1277 N: 1254	A: 1747 N: 1753	A: 1224 N: 1224	1095	(T) Hoagy is a synonym of an italian sandwich. (Fa) Decalogue is an astronomer. (S) Dostab is a scencer. (Fi) Snozberry is a type of a berry.

[†] A version of this table without the Fictional and Noise columns can be found in [12].

particular relevance is the **sAwMIL** framework [12], which uses multiple-instance learning and conformal prediction to classify statements as **True**, **False**, or **Neither**. Hallucination-detection studies likewise suggest that hidden states encode strong veracity signals even when outputs are incorrect [3]. These empirical approaches complement philosophical work clarifying when neural components should count as representations [18].

A separate line of research demonstrates that LLM outputs are highly sensitive to prompting and context. Models are vulnerable to jailbreaks [17], sycophancy [23], word variation [8], and multi-turn drift [9]. These studies diagnose behavioral brittleness rather than instability in the underlying representations, though recent evidence on epistemic familiarity suggests that some output-level failures may trace back to deeper weaknesses in internal epistemic structure [10].

LLMs also struggle to distinguish between belief, knowledge, and fact. Suzgun et al. [5] show that LLMs often fail to track agents’ beliefs when those beliefs are mistaken, underscoring weaknesses in their epistemic structure. Uncertainty-focused analyses reveal similar failures under epistemic ambiguity, i.e., when information admits multiple plausible interpretations [6]. Theoretical work also argues that the study of LLM beliefs lacks unified standards, with Herrmann and Levinstein proposing criteria for when internal states should count as belief-like [24]. Formal epistemology offers a complementary perspective: Leitgeb’s theory of P -stability links rational belief to stable truth assignments under small contextual changes [19]. This connection motivates our focus on representational stability as an epistemic property of model activations rather than model outputs.

We bridge probing and in-context work by measuring how controlled label perturbations reshape inferred truth directions, thereby identifying which types of familiar and unfamiliar **Neither** statements most strongly disrupt an LLM’s latent encoding of veracity.

3 Methodology

We treat an LLM’s internal activations as a proxy for its belief structure and use the decision boundary learned by a linear probe as a geometric diagnostic of how truth is encoded in that space. We define *representational stability* as the consistency of this boundary under controlled perturbations of what counts as **True** (see Fig. 1). The notation introduced in this section is summarized in Supplementary Table A1.

Statements and Labels. We begin with a collection of statements $\mathcal{S} = \{s_i\}_{i=1}^N$ drawn from factual domains. Each statement has a ground-truth veracity label $y_i \in \{\text{True}, \text{False}, \text{Neither}\}$. The **Neither** category includes familiar **Fictional** statements (e.g., “*Gotham City is in New Jersey*”) and unfamiliar **Synthetic** fact-like statements (e.g., “*The city of Norminsk is located in Jamoates*”).

Activation Extraction. Each statement s_i is passed through an LLM \mathcal{M} to obtain its internal activation $\mathbf{z}_i^{(l)}$ a layer l , chosen empirically to maximize linear separability between **True** and **Not True** statements [11, 12, 13]. These activations constitute the model’s *veracity representations*. We construct the dataset

$$\mathcal{D} = \{(\mathbf{z}_i^{(l)}, y_i)\}_{i=1}^N,$$

and partition it into training, calibration, and test splits: $\mathcal{D}_{\text{train}}$, \mathcal{D}_{cal} , and $\mathcal{D}_{\text{test}}$.

Baseline Probe Training. We train a max-margin, multiple-instance probe \mathcal{P} (namely, **sAwMIL** [12]) that learns a linear decision boundary $f(\mathbf{z}) = \vec{w} \cdot \mathbf{z} + b$, where \vec{w} represents the *truth direction*. Labels are encoded as $y'_i \in \{+1, -1\}$:

$$y'_i = \begin{cases} +1, & \text{if } y_i = \text{True} \\ -1, & \text{if } y_i = \text{Not True} \end{cases}$$

Table 2. Label configurations for experiments. Each row defines the composition of the **True** and **Not True** classes used when retraining the probe under different perturbation conditions. The baseline (Original) probe is trained on **True** statements versus all others, while perturbed probes redefine the **True** class to include additional statement types to test representational stability under shifts in the operational definition of truth. **Fictional(T)** denotes fictional truth and **Fictional(F)** denotes fictional falsehood.

	Perturbation Type	Statements Considered True	Statements Considered Not True
Original	Baseline	True	False + Synthetic + Fictional + Noise
Perturbed	Synthetic	True + Synthetic	False + Fictional + Noise
	Fictional	True + Fictional	False + Synthetic + Noise
	Fictional(T)	True + Fictional(T)	False + Synthetic + Fictional(F) + Noise
	Noise	True + Noise	False + Synthetic + Fictional

Training on $\mathcal{D}_{\text{train}}$ yields the baseline classifier. The set of statements that the probe, and by extension the LLM’s latent geometry, represents as **True** is

$$\mathcal{B}_{\text{true}} = \{s_i \mid \mathbf{z}_i^{(l)} \in \mathcal{D}_{\text{test}}, y_i = \text{True}, \hat{y}_i = +1\}.$$

We interpret $\mathcal{B}_{\text{true}}$ as the model’s baseline belief set under the original definition of truth.

Label Perturbations and Retraining. To assess representational stability, we systematically vary which **Neither** statements are treated as **True**. Let \mathcal{N} denote all **Neither** statements and partition it into two subsets \mathcal{N}_1 and \mathcal{N}_0 , such that

$$\mathcal{N} = \mathcal{N}_1 \cup \mathcal{N}_0, \quad \mathcal{N}_1 \cap \mathcal{N}_0 = \emptyset.$$

Relabeling \mathcal{N}_1 as **True** and \mathcal{N}_0 as **Not True** yields the perturbed labels

$$y''_i = \begin{cases} +1, & \text{if } y_i \in \{\text{True}\} \cup \mathcal{N}_1, \\ -1, & \text{if } y_i \in \{\text{False}\} \cup \mathcal{N}_0. \end{cases}$$

Using the same data splits, we retrain the probe to obtain (\vec{w}', b') and define the perturbed belief set as

$$\mathcal{B}'_{\text{true}} = \{s_i \mid \mathbf{z}_i^{(l)} \in \mathcal{D}_{\text{test}}, y_i = \text{True}, \hat{y}'_i = +1\}.$$

Comparing $\mathcal{B}_{\text{true}}$ and $\mathcal{B}'_{\text{true}}$ reveals how the probe’s truth assignments shift under modified semantic assumptions while the underlying LLM activations remain fixed.

Quantifying Representational Stability. Stability is quantified in two complementary ways. First, we measure geometric stability by comparing the decision boundaries (\vec{w}, b) and (\vec{w}', b') . Cosine similarity between \vec{w} and \vec{w}' captures rotational changes in the truth direction, while $|b - b'|$ captures translational shifts of the hyperplane.

Second, we evaluate prediction stability by comparing belief sets:

$$\begin{aligned} \mathcal{B}_{\text{true}} \cap \mathcal{B}'_{\text{true}} & \quad (\text{stable truths}), \\ \mathcal{B}_{\text{true}} \setminus \mathcal{B}'_{\text{true}} & \quad (\text{epistemic retractions}), \\ \mathcal{B}'_{\text{true}} \setminus \mathcal{B}_{\text{true}} & \quad (\text{epistemic expansions}). \end{aligned}$$

Following P -stability theory [19], retractions indicate stronger instability because they withdraw beliefs, whereas expansions reflect milder over-inclusiveness.

Together, these measures assess how reliably the LLM’s veracity representations support stable truth assignments under shifts in semantic boundaries. The probe’s decision boundary thus serves not as an end task, but as a geometric lens on how belief, falsity, and plausibility are structured within the LLM’s activation space.

4 Experiments

4.1 Data

Our experiments draw on the three factual domains introduced in [12]: *City Locations*, *Medical Indications*, and *Word Definitions*. Although all three domains contain factual assertions, they differ in how sharply truth and falsehood are delineated. Statements in *City Locations* are objective and stable. Statements in *Medical Indications* are factual but context-dependent. Statements in *Word Definitions* are more interpretive due to polysemy and variation in usage. This range provides a diverse testbed for studying how LLMs encode veracity across domains. Full dataset construction and validation details appear in Supplementary Section B.

We analyze five types of statements: **True**, **False**, **Synthetic**, **Fictional**, and **Noise** (Table 1). We take the **True**, **False**, and **Synthetic** statements directly from [12]. **Synthetic** statements are grammatically coherent but semantically meaningless constructions built from generated entity names. Because these entities cannot have appeared in training corpora, LLMs lack the background needed to assign them a truth value. They therefore serve as unfamiliar **Neither** statements for which calibrated models should suspend belief.

Fictional statements lack real-world truth value.¹ Unlike unfamiliar **Synthetic** statements, many fictional entities (e.g., *Gotham City*, *Xenovirus Takis-B*) are likely present in training corpora. **Fictional** statements test

¹We have released the fictional statements at https://huggingface.co/datasets/samanthadies/representational_stability.

Distribution of 2-grams (Smoothed)

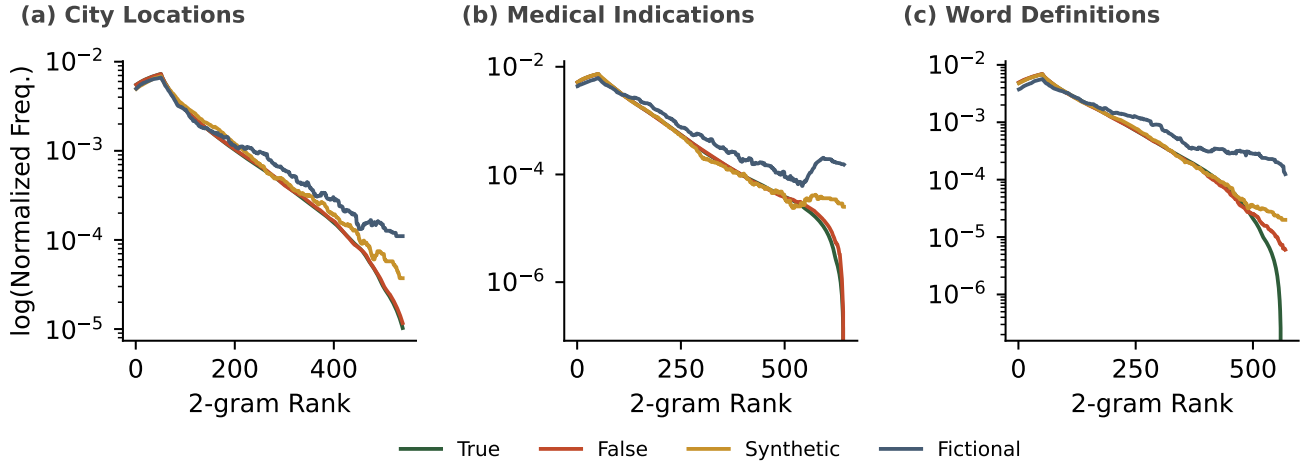


Figure 2. Character bigram distributions of statements. Rank–frequency plots of normalized character bigram counts for True (green), False (red), Synthetic (yellow), and Fictional (blue) statements in the (a) City Locations, (b) Medical Indications, and (c) Word Definitions datasets. For each dataset, we compute per-type bigram frequencies, normalize within type, sort bigrams by their frequency under True statements, and plot log-normalized frequency with a moving-average smoothing. Across datasets, the True, False, and Synthetic distributions are nearly indistinguishable, whereas the Fictional distribution decays more slowly, marking it as structurally distinct.

whether LLMs distinguish between *recognition* and *factual commitment*: a model may have rich associations with these entities while still treating them as nonfactual.

Finally, **Noise** serves as a non-semantic control. We sample random activation sequences matched to the mean, variance, and sequence-length distribution of the real activations. This ensures that observed representational effects arise from semantic content and context rather than from activation-space statistics alone.

4.2 Stability

We measure stability to discuss the probe, the activations, and the perturbations.

Probe. We use the sparse-aware multiple-instance learning probe (**sAwMIL**) [12], a multiclass probing method designed to extract reliable and transferable veracity directions from LLM activations. Unlike simpler probes such as the **Mean Difference** classifier [13], which assumes that truth and falsehood lie along a single axis, **sAwMIL** models **True**, **False**, and **Neither** as distinct directions and aggregates token-level representations using multiple-instance learning. It also incorporates conformal prediction [25] to calibrate uncertainty. As a max-margin method, **sAwMIL** yields stable decision boundaries, making differences across perturbations more reflective of genuine structure in the LLM’s geometry than probe noise. For comparison, results from the **Mean Difference** probe appear in Supplementary Section E.

Generating and Characterizing Activations. We consider sixteen open-source LLMs spanning the Gemma, Llama, Mistral, and Qwen families, with both base and chat-tuned variants (see Supplementary Section C). For each \langle dataset, LLM \rangle pair, we extract token-level activations from the layer that maximizes linear separability between **True** and **Not True** statements [12] (see Supplementary Table A3). We then record the sequence of hidden states $\mathbf{z}_i^{(l)}$ for each statement s_i .

For descriptive, model-agnostic analyses, we reduce each sequence to a single vector by selecting the final non-padding token. We then characterize patterns at both the linguistic and representation levels. At the linguistic level, we compute rank–frequency curves over character bigrams aggregated across entity names for each statement type. At the representation level, we compute pairwise 1-D Wasserstein distances between activation distributions across all dimensions, averaged across LLMs. These metrics reveal similarities between statement types at the linguistic level and in latent space before any supervised probing.

Perturbations. For each \langle dataset, LLM \rangle pair, we train one baseline probe and four perturbed probes as listed in Table 2.² In the **Baseline** condition, **True** statements are contrasted with all others. The **Synthetic** pertur-

²We also evaluated perturbations in which each **Neither** type was added separately to either the **True** or **False** class. We observed qualitatively similar results.

Wasserstein Distance between Activations (Averaged over LLMs)

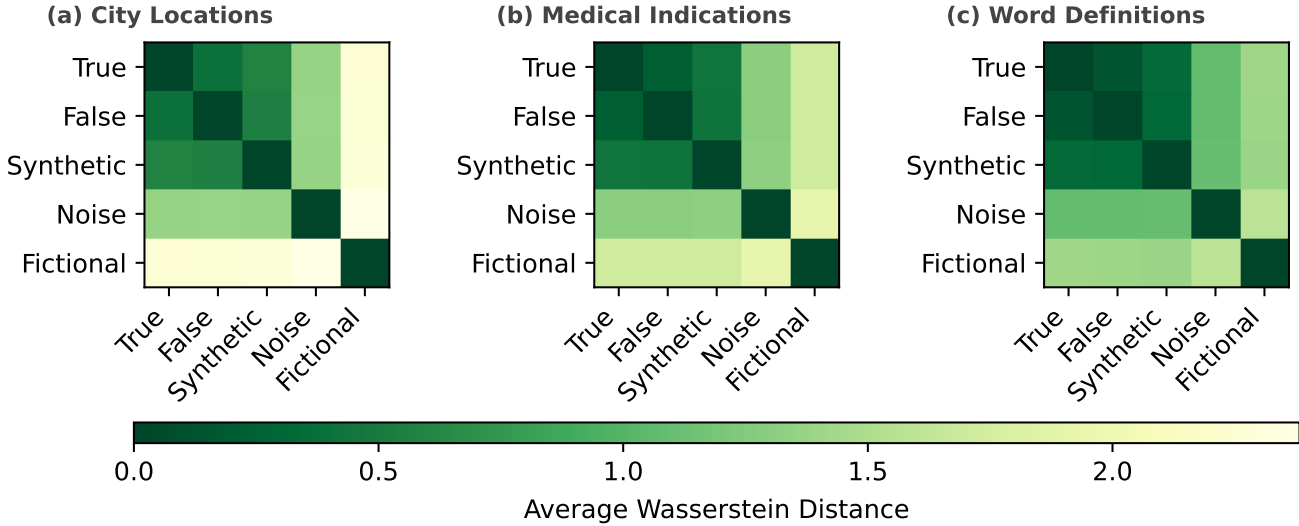


Figure 3. Average Wasserstein distance between activations. Pairwise Wasserstein distances between activation distributions of True, False, Synthetic, Fictional, and Noise statements, averaged over sixteen LLMs for the (a) City Locations, (b) Medical Indications, and (c) Word Definitions datasets. Across datasets, Synthetic activations lie closest to the True and False activations, while Fictional and Noise activations are farther from all others, indicating that unseen but fact-like statements (Synthetic) resemble factual structure, whereas Fictional statements form distinct representational clusters.

bation treats True and Synthetic as True, testing how unfamiliar fact-like content shifts the decision boundary. The Fictional perturbation treats True and Fictional as True, testing the influence of linguistically familiar but nonfactual content. The Fictional (T) perturbation further separates Fictional statements by canonical truth (e.g., “*Smallville is located in Kansas*” vs. “*Smallville is located in Virginia*”). Finally, the Noise perturbation treats True and Noise as True, serving as a sanity check in which the added truths are random Gaussian activations rather than semantic content.

Experimental Details. Activation sequences, data splits, hyperparameters, and preprocessing steps are held fixed. Token-level representations are scaled using a standard scaler fit on the training set; bags are truncated to a fixed maximum size; and we perform a small grid search over the regularization parameter C using three-fold cross-validation with mean average precision as the criterion. Approximately 55% of the data is used for training, 20% for calibration, and 25% for testing (see Supplementary Table A2). Holding all training conditions constant ensures that changes in the learned truth direction arise solely from label perturbations.

5 Results

We present results at three levels of analysis. First, we examine the *input representations*: how statement types

differ in linguistic-level features and in activation space. Second, we measure *probe-level changes* by assessing how the learned True vs. Not True direction shifts under controlled label perturbations. Third, we analyze *output-level changes* in the probe’s predicted labels, quantifying how truth-value assignments respond to modified semantic assumptions.

5.1 Representations of True, False, and Neither Statements

We first characterize the probe inputs. At the linguistic level, True, False, and Synthetic statements exhibit nearly identical normalized bigram distributions across all three domains (Figure 2). This confirms that the generation procedure for Synthetic statements³ preserves low-level linguistic structure. Fictional statements, however, show a slower rank–frequency decay, reflecting stylistic patterns characteristic of narrative text. This divergence is most visible in Word Definitions (Fig. 2(c)) and least visible in City Locations (Fig. 2(a)), where some fictional cities align with real countries (e.g., “*Brigadoon is located in Scotland*”).

We next test whether these linguistic-level differences correspond to differences in latent space by computing pairwise Wasserstein distances between activation distributions for all statement types (Fig. 3; per-model

³See Supplementary B.1.1 for details on the procedure that generates Synthetic statements.

Change in sAwMIL Decision Boundary under Perturbations

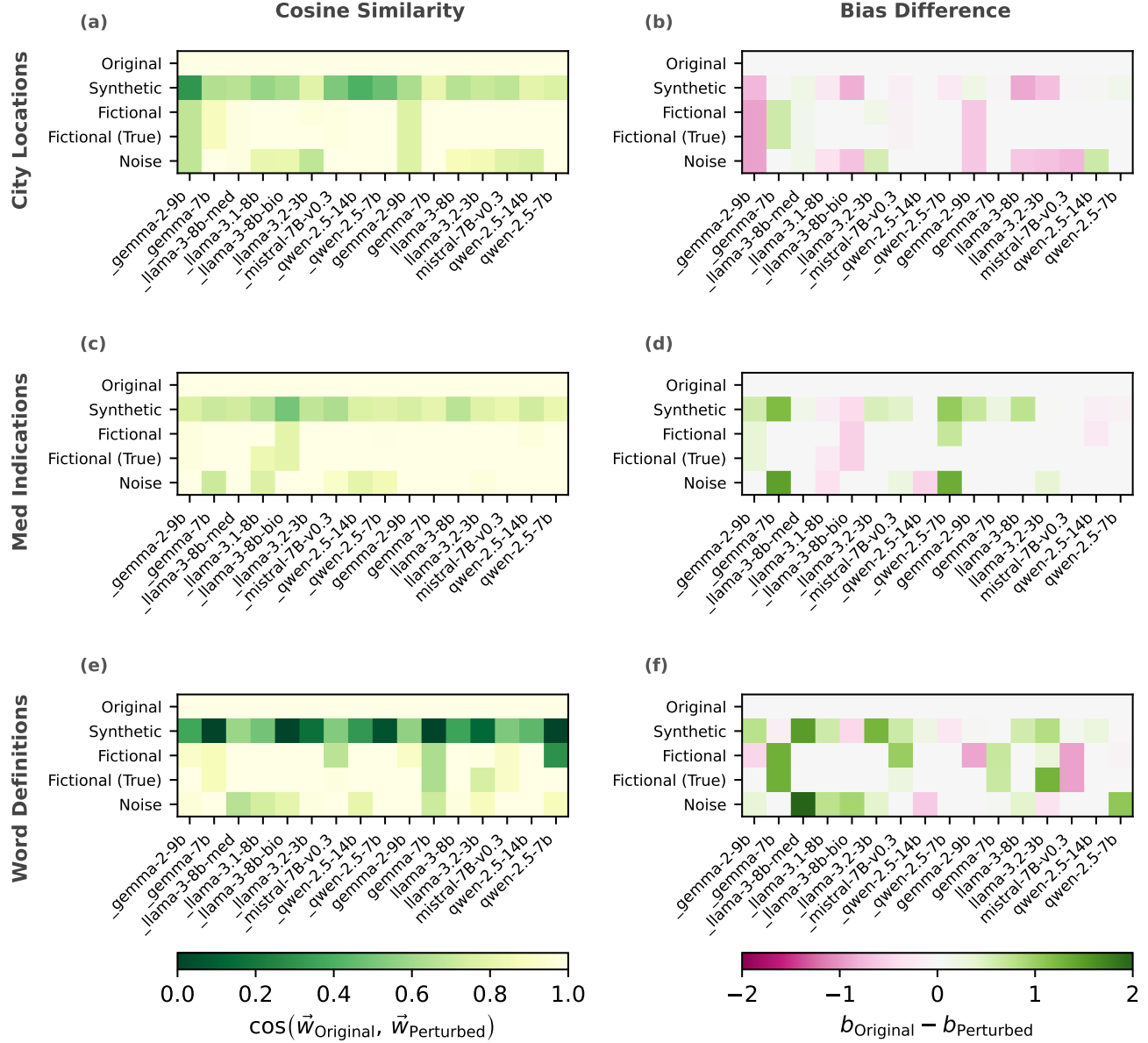


Figure 4. Changes in the probe decision boundary under perturbations. Cosine similarity (left column) and bias difference (right column) between the baseline True vs. Not True probe and probes retrained under label perturbations for the (a,b) City Locations, (c,d) Medical Indications, and (e,f) Word Definitions datasets. Each heatmap shows results for sixteen LLMs (columns) and five perturbation conditions (rows). LLMs with leading underscores are chat models, while those without are base models. Higher cosine similarity indicates smaller rotations of the learned decision boundary, while bias difference reflects shifts in intercept. Across datasets, probes retrained with the **Synthetic** perturbation show the largest deviation from the original, particularly in cosine similarity.

Table 3. Flipped predictions under label perturbations. Counts (and percentages) of predictions that remain stable or flip between True and Not True across Synthetic, Fictional, Fictional(T), and Noise perturbations for each dataset. City Locations is the most stable, with only 4.8% of statements flipping in the worst case, followed by Medical Indications (12.2%) and Word Definitions (40.6%). Across all domains, Synthetic perturbations produce the most flips, suggesting that unseen but fact-like statements most strongly distort the learned veracity boundaries.

Dataset	Perturbation	True to True	Not True to Not True	Not True to True	True to Not True	Total Flips
City Locations	Synthetic	9153 (91.5)	360 (3.6)	274 (2.7)	213 (2.1)	460 (4.8)
	Fictional	9326 (93.3)	568 (5.7)	66 (0.7)	40 (0.4)	106 (1.1)
	Fictional (T)	9330 (93.3)	576 (5.8)	58 (0.6)	36 (0.4)	94 (1.0)
	Noise	9183 (91.8)	532 (5.3)	102 (1.0)	183 (1.8)	285 (2.8)
Medical Locations	Synthetic	7413 (72.6)	1556 (15.2)	786 (7.7)	460 (4.5)	1246 (12.2)
	Fictional	7808 (76.4)	2284 (22.4)	58 (0.6)	65 (0.6)	131 (1.3)
	Fictional (T)	7815 (76.5)	2269 (22.2)	73 (0.7)	58 (0.6)	427 (1.3)
	Noise	7779 (76.2)	2009 (19.7)	333 (3.3)	94 (0.9)	427 (4.2)
Word Definitions	Synthetic	3682 (37.2)	2188 (22.1)	785 (7.9)	3233 (32.7)	4018 (40.6)
	Fictional	6507 (65.8)	2494 (25.2)	479 (4.1)	408 (4.1)	887 (8.2)
	Fictional (T)	6795 (68.7)	2520 (25.5)	453 (4.6)	120 (1.2)	573 (5.8)
	Noise	6653 (67.3)	2251 (25.4)	462 (4.7)	262 (2.6)	724 (7.3)

City Locations: Changes in Predicted Labels by Model (Given $y = \text{True}$)

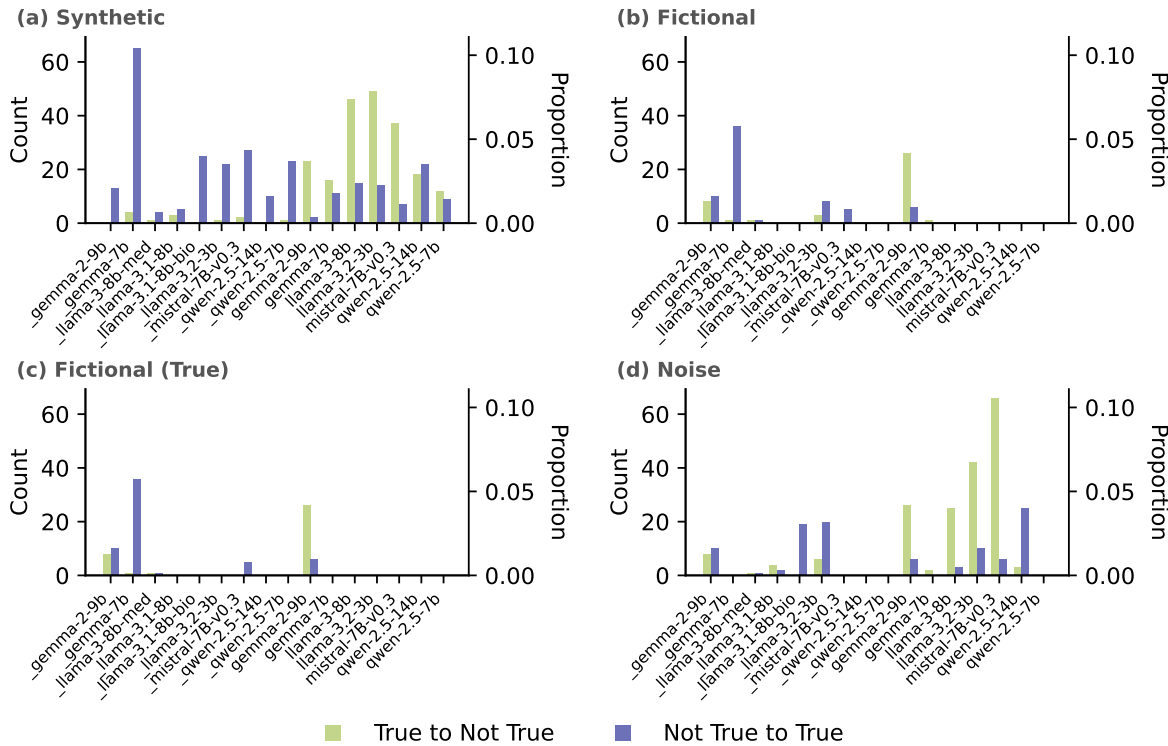


Figure 5. Stability of probe predictions under label perturbations for City Locations data. Bar plots show, for each of the sixteen LLMs (x-axis), how often the sAwMIL probe’s predicted label changes when retrained under four perturbations: (a) Synthetic, (b) Fictional, (c) Fictional(T), and (d) Noise. Green bars indicate True to Not True flips, while purple bars indicate Not True to True flips. The left y-axis reports the number of statements with flipped predictions, and the right y-axis reports the corresponding proportions. The Synthetic perturbation leads to the most instability, and the base models exhibit more True to Not True flips than the chat models.

Med. Indications: Changes in Predicted Labels by Model (Given $y = \text{True}$)

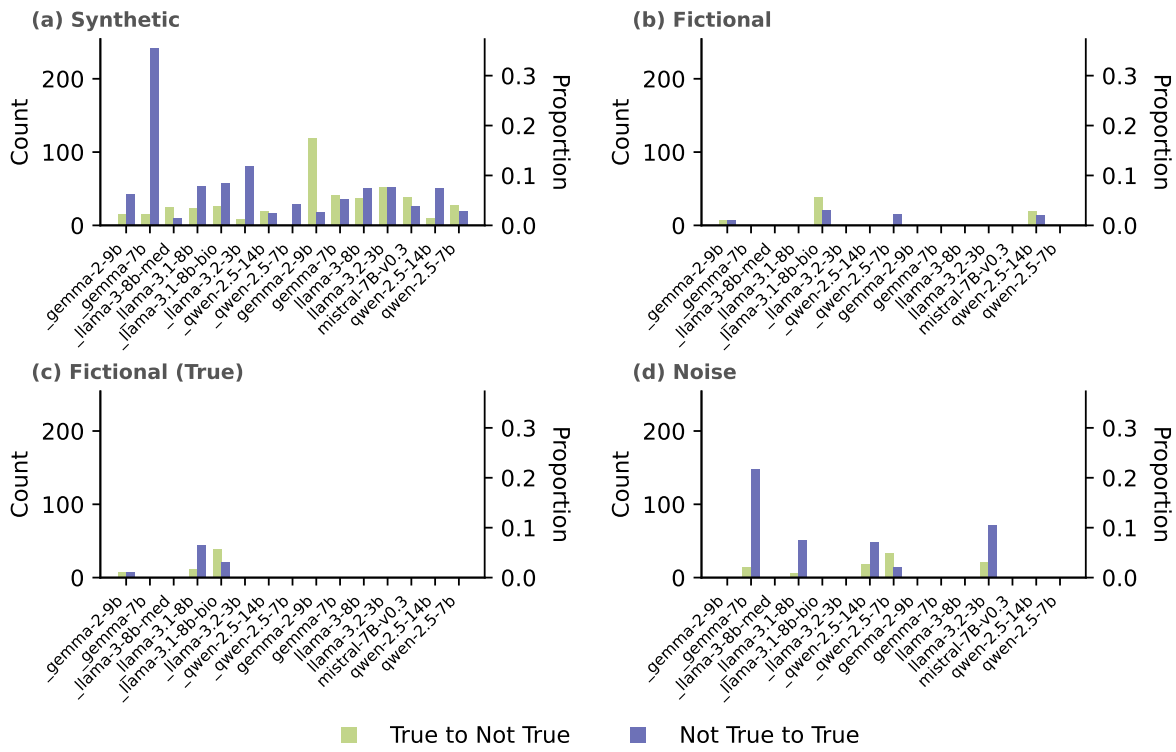


Figure 6. Stability of probe predictions under perturbations for Medical Indications data. Bar plots show, for each of the sixteen LLMs (x-axis), how often the sAwMIL probe’s predicted label changes when retrained under four perturbations: (a) Synthetic, (b) Fictional, (c) Fictional(T), and (d) Noise. Green bars indicate True to Not True flips, while purple bars indicate Not True to True flips. The left y-axis reports the number of statements with flipped predictions, and the right y-axis reports the corresponding proportions. The Synthetic perturbation leads to the most instability, and the Fictional and Fictional(T) perturbations result in almost no flips.

heatmaps appear in Supplementary Figures A1–A16).

Across all sixteen LLMs, True and False representations lie close together, with mean distances of 0.40, 0.29, 0.14 for City Locations, Medical Indications, and Word Definitions, respectively.

Synthetic statements remain only modestly farther from **True**, with mean distances of 0.58, 0.44, 0.33 for City Locations, Medical Indications, and Word Definitions, respectively. This is consistent with their linguistic similarity despite their unfamiliarity.

By contrast, **Fictional** and **Noise** statements lie much farther from **True**. For **Fictional**, the mean distances from **True** are 2.28, 1.30, 1.41 for City Locations, Medical Indications, and Word Definitions, respectively. For **Noise**, the mean distances from **True** are 1.37, 1.30, 1.09 for City Locations, Medical Indications, and Word Definitions, respectively. The mean distances between **Fictional** and **Noise** are 2.38, 1.93, 1.58 for City Locations, Medical Indications, and Word Definitions, respectively. **Fictional** statements form

their own representational cluster shaped not only by lexical differences but by their appearance in non-factual contexts during training.

Taken together, these findings **show a clear decoupling between linguistic and latent-space similarity**. Word Definitions exhibit substantial linguistic divergence between factual and fictional content, yet only moderate activation-space divergence. Conversely, City Locations show minimal linguistic differences but large representational separation. The geometry of LLM activations thus reflects both linguistic form and epistemic context.

5.2 Probe-level Changes under Label Perturbations

We assess representational stability by retraining the probe with expanded definitions of **True** (i.e., by treating **Synthetic**, **Fictional**, **Fictional(T)**, or **Noise** as **True**). Because the LLM activations remain fixed, shifts in the learned boundary reflects how the underlying veracity structure supports (or resists) linear reclassification.

Word Definitions: Changes in Predicted Labels by Model (Given $y = \text{True}$)

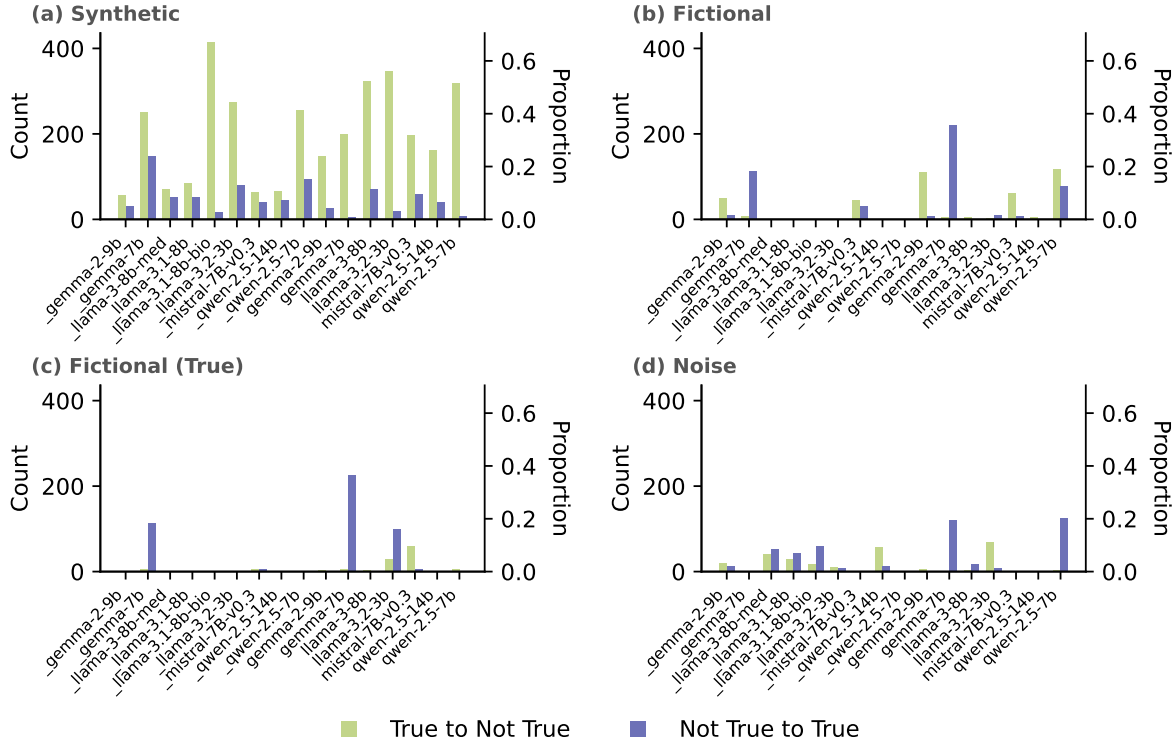


Figure 7. Stability of probe predictions under label perturbations for Word Definitions data. Bar plots show, for each of the sixteen LLMs (x-axis), how often the sAwMIL probe’s predicted label changes when retrained under four perturbations: (a) Synthetic, (b) Fictional, (c) Fictional (True), and (d) Noise. Green bars indicate True to Not True flips, while purple bars indicate Not True to True flips. The left y-axis reports the number of statements with flipped predictions, and the right y-axis reports the corresponding proportions. The Synthetic perturbation leads to the most instability, with some LLMs retracting over 50% of their originally True statements.

Figure 4 reports cosine similarity and intercept shifts between baseline and perturbed classifiers. Cosine similarity captures rotations of the True vs. Not True direction, while bias differences capture translational shifts. Across the datasets, Synthetic perturbations induce the largest boundary rotations, often nearing orthogonality in Word Definitions (Fig. 4(e),(f)). Fictional and Noise perturbations yield considerably smaller deviations. These results indicate that the baseline True vs. Not True direction is generally stable, but that adding unfamiliar yet semantically factual statements forces substantial reorientation. Synthetic statements therefore reveal where the veracity structure is most brittle.

Although the global pattern is consistent, different LLM families exhibit different degrees of susceptibility to these perturbations. Chat-tuned variants (denoted by leading underscores) tend to exhibit somewhat larger rotations and bias shifts than their base models. An exception is gemma-7b, which shows unusually large shifts in the Word Definitions domain. Importantly, such ro-

tations do not necessarily imply failures of predictive accuracy: large re-orientations can reflect either weak separation or greater dispersion within the underlying latent geometry (e.g., models with larger inter-type Wasserstein distances). Overall, across models and domains, Synthetic perturbations consistently produce the strongest probe-level instability.

5.3 Changes in Predicted Labels

We examine how shifts in the truth boundary affect predicted veracity labels. Table 3 reports the percentage of statements whose predicted labels remain stable versus those that flip between True and Not True. City Locations is most stable (maximum flip rate 4.8%), Medical Indications shows intermediate instability (12.2%), and Word Definitions is substantially less stable (up to 40.6%). In all domains, Synthetic perturbations yield the highest flip rates, reinforcing that unfamiliar yet semantically fact-like statements are most disruptive to the learned veracity boundary.

Figures 5–7 show flip patterns by model family.

Chat-tuned models tend to produce more **Not True** to **True** flips, suggesting a mild tendency toward over-inclusiveness when the **True** class expands. Base models tend to show the opposite pattern. From a P -stability perspective, **True** to **Not True** flips represent stronger epistemic instability, as they retract previously assigned beliefs. However, these tendencies do not hold uniformly, and overall differences across LLM families are smaller than differences across perturbation types.

Taken together, these output-level results **reveal a consistent hierarchy of representational stability**. Domains richly represented in training corpora (e.g., geography) exhibit the strongest representational stability; specialized but widely discussed domains (e.g., medicine) show moderate stability; and semantically flexible domains (e.g., definitions) are most vulnerable. Across all cases, **Synthetic** perturbations remain the dominant source of instability, indicating that unfamiliar yet factually plausible statements impose the greatest challenge for generating well-organized truth representations in LLMs.

6 Discussion

Our results show that LLMs encode a coherent but sometimes brittle separation of veracity in their internal activations. **True**, **False**, and familiar **Fictional** statements form well-defined clusters, while unfamiliar **Synthetic** statements sit near the boundary and disrupt it when relabeled as **True**. Because the activations remain fixed, these disruptions reflect genuine weaknesses in the underlying veracity geometry rather than artifacts of training or optimization. The mismatch between linguistic similarity and activation-space similarity across domains further indicates that representational stability is driven by epistemic familiarity, not linguistic-level features.

A central implication is that representational stability depends strongly on *training-induced familiarity*. Familiar **Fictional** statements appear in narrative contexts the LLMs have likely repeatedly encountered, enabling them to form stable, internally coherent clusters. Unfamiliar **Synthetic** statements lack any such anchoring: they resemble factual claims but violate the LLM’s learned priors. As a result, they induce the largest rotations and label flips, mirroring how humans show greater belief instability when confronted with novel but superficially plausible assertions. In this way, the probe’s decision boundary serves as a diagnostic of the model’s epistemic landscape, revealing which statements the model encodes as grounded, merely recognized, or unsupported.

Domain differences reinforce this picture. City Locations, which are richly represented and highly regular in training data, shows the tightest clustering and highest stability. Medical Indications, which are factual but context-sensitive, shows moderate stability. Word Definitions, which are semantically flexible and often usage-

dependent, show the weakest structure. This reflects broader patterns in factual generalization: LLMs inherit the uneven epistemic structure of their training corpora, and their capacity to encode veracity varies accordingly.

Beyond characterizing these patterns, our method helps diagnose the representational sources of factual inconsistency. By perturbing the labeling of truth rather than modifying LLM parameters, we isolate which semantic shifts the underlying geometry will tolerate. This complements output-based factuality metrics: rather than asking whether a model *states* the truth, we evaluate whether it *represents* truth in a stable, well-organized fashion. Such diagnostics could guide data curation, fine-tuning objectives, or auditing procedures focused on improving epistemic reliability rather than linguistic-level accuracy.

Finally, our results connect to philosophical accounts of P -stability [19], which hold that rational beliefs should remain stable under small evidential changes. In our setting, reclassifying **Neither** statements that are logically consistent with the **True** statements should preserve the inferred truth boundary if the model’s epistemic representation is robust. Instead, **Synthetic** perturbations cause substantial reorientation. This highlights a deeper challenge: distributional similarity alone does not guarantee that truth, falsity, and indeterminacy are encoded in forms that support stable inference. Addressing this may require training objectives or architectures that explicitly distinguish these epistemic categories.

Future Work. Our analysis focuses on representational (and not behavioral) stability. We evaluate how truth directions emerge from fixed activations rather than how LLMs revise beliefs. Extending the framework to dynamic settings, such as after fine-tuning, reinforcement learning, or conversational interaction, may reveal how representational shifts propagate to behavior. Although **sAwMIL** [12] provides a strong linear diagnostic, non-linear or causal probes could uncover subtler dependencies among veracity, uncertainty, and linguistic form. Finally, our datasets center on factual and quasi-factual content; applying the method to disputed, opinion-based, counterfactual, or evolving claims would broaden the range of epistemic ambiguity and deepen our understanding of how LLMs encode belief.

7 Conclusion

This study introduces *representational stability* as an approach for examining how LLMs internally encode and preserve distinctions between **True**, **False**, and **Neither** statements. By combining controlled label perturbations with a representation-based probe, we show that LLMs display a coherent but uneven geometry of truth. Factual representations are generally well structured, but plausible yet not **True** statements unseen during training (i.e.,

unfamiliar **Synthetic** Neither statements) most readily disrupt that structure. These effects are consistent across architectures and domains, revealing that **epistemic familiarity of the LLM with the content, rather than linguistic similarity or model scale, determines the stability of veracity representations.** These findings underscore the importance of evaluating not only what LLMs output, but also the reliability of the veracity representations. Understanding and reinforcing this internal coherence offers a path toward models that are not only accurate in response but also epistemically stable in representation.

Acknowledgments

We thank Hannes Leitgeb and Branden Fitelson for discussions on *P*-stability and how it might be related to epistemic uncertainty in LLMs. We also thank Zohair Shafi and Moritz Laber for their feedback and discussions on methodological and empirical portions of this work.

Funding

This work was supported in part by DOD CDAO funds, which we received through Carnegie Mellon University's Software Engineering Institute.

Competing interests

The authors declare no competing interests.

Data availability

True, False, and Synthetic statements are available at <https://huggingface.co/datasets/carlomarxx/trilemma-of-truth>. Fictional statements are available at https://huggingface.co/datasets/samanthadies/representational_stability. The code used to generate the Noise activations can be found at https://github.com/samanthadies/representational_stability.

Code availability

The code used to generate activations, generate the Noise activations, and run the stability experiments can be found at https://github.com/samanthadies/representational_stability.

References

1. AlKhamissi, B., Li, M., Celikyilmaz, A., Diab, M. & Ghazvininejad, M. A review on language models as knowledge bases. *arXiv preprint arXiv:2204.06031* <https://doi.org/10.48550/arXiv.2204.06031> (2022).
2. Turpin, M., Michael, J., Perez, E. & Bowman, S. Language models don't always say what they think: Unfaithful explanations in Chain-of-Thought prompting. *Adv. Neural Inf. Process. Syst.* **36**, 74952–74965 (2023).
3. Han, J. *et al.* Simple factuality probes detect hallucinations in long-form natural language generation. In Christodoulopoulos, C., Chakraborty, T., Rose, C. & Peng, V. (eds.) *Findings of the Association for Computational Linguistics: EMNLP 2025*, 16209–16226. <https://doi.org/10.18653/v1/2025.findings-emnlp.880> (Association for Computational Linguistics, 2025).
4. Liu, Y. *et al.* Trustworthy LLMs: a survey and guideline for evaluating large language models' alignment. In *Socially Responsible Language Modelling Research*. <https://doi.org/10.48550/arXiv.2308.05374> (2023).
5. Suzgun, M. *et al.* Language models cannot reliably distinguish belief from knowledge and fact. *Nat. Mach. Intell.* 1–11. <https://doi.org/10.1038/s42256-025-01113-8> (2025).
6. Abbasi Yadkori, Y., Kuzborskij, I., György, A. & Szepesvari, C. To believe or not to believe your LLM: Iterative prompting for estimating epistemic uncertainty. *Adv. Neural Inf. Process. Syst.* **37**, 58077–58117 (2024).
7. Huang, L. *et al.* A survey on hallucination in large language models: Principles, taxonomy, challenges, and open questions. *ACM Transactions on Inf. Syst.* **43**, 1–55. <https://doi.org/10.1145/3703155> (2025).
8. Elazar, Y. *et al.* Measuring and improving consistency in pretrained language models. *Transactions Assoc. for Comput. Linguist.* **9**, 1012–1031. https://doi.org/10.1162/tacl_a_00410 (2021).
9. Li, Y., Miao, Y., Ding, X., Krishnan, R. & Padman, R. Firm or fickle? evaluating large language models consistency in sequential interactions. *arXiv preprint arXiv:2503.22353* <https://doi.org/10.48550/arXiv.2503.22353> (2025).
10. Kadavath, S. *et al.* Language models (mostly) know what they know. *arXiv preprint arXiv:2207.05221* (2022).
11. Bürger, L., Hamprecht, F. A. & Nadler, B. Truth is universal: Robust detection of lies in LLMs. *Adv. Neural Inf. Process. Syst.* **37**, 138393–138431 (2024).
12. Savcisen, G. & Eliassi-Rad, T. Trilemma of truth in large language models. In *Mechanistic Interpretability Workshop at NeurIPS 2025* (2025). <https://openreview.net/forum?id=z7dLG2ycRf>.

13. Marks, S. & Tegmark, M. The geometry of truth: Emergent linear structure in large language model representations of True/False datasets. *arXiv preprint arXiv:2310.06824* <https://doi.org/10.48550/arXiv.2310.06824> (2024).
14. Wilie, B., Cahyawijaya, S., Ishii, E., He, J. & Fung, P. Belief revision: The adaptability of large language models reasoning. *arXiv preprint arXiv:2406.19764* <https://doi.org/10.48550/arXiv.2406.19764> (2024).
15. Xu, R. *et al.* The earth is flat because...: Investigating LLMs' belief towards misinformation via persuasive conversation. In Ku, L.-W., Martins, A. & Sriku-mar, V. (eds.) *Proceedings of the 62nd Annual Meeting of the Association for Computational Linguistics (Volume 1: Long Papers)*, 16259–16303. <https://doi.org/10.18653/v1/2024.acl-long.858> (2024).
16. Lu, Y., Bartolo, M., Moore, A., Riedel, S. & Sten-
torp, P. Fantastically ordered prompts and where to find them: Overcoming few-shot prompt order sensitivity. In *Proceedings of the 60th Annual Meeting of the Association for Computational Linguistics (Volume 1: Long Papers)*, 8086–8098. <https://doi.org/10.18653/v1/2022.acl-long.556> (2022).
17. Wei, A., Haghtalab, N. & Steinhardt, J. Jailbroken: How does LLM safety training fail? *Adv. Neural Inf. Process. Syst.* **36**, 80079–80110 (2023).
18. Harding, J. Operationalising representation in natural language processing. *Br. J. for Philos. Sci.* <https://doi.org/10.1086/728685> (2023).
19. Leitgeb, H. The stability theory of belief. *Philos. review* **123**, 131–171. <https://doi.org/10.1215/00318108-2400575> (2014).
20. Conneau, A., Kruszewski, G., Lample, G., Barrault, L. & Baroni, M. What you can cram into a single vector: Probing sentence embeddings for linguistic properties. *arXiv preprint arXiv:1805.01070* <https://doi.org/10.48550/arXiv.1805.01070> (2018).
21. Hewitt, J. & Manning, C. D. A structural probe for finding syntax in word representations. In *Proceedings of the 2019 Conference of the North American Chapter of the Association for Computational Linguistics: Human Language Technologies, Volume 1 (Long and Short Papers)*, 4129–4138. <https://doi.org/10.18653/v1/N19-1419> (2019).
22. Tenney, I., Das, D. & Pavlick, E. Bert rediscovers the classical nlp pipeline. In *Association for Computational Linguistics*. <https://doi.org/10.48550/arXiv.1905.05950> (2019).
23. Sharma, M. *et al.* Towards understanding sycophancy in language models. In *The Twelfth International Conference on Learning Representations*. <https://doi.org/10.48550/arXiv.2310.13548> (2024).
24. Herrmann, D. A. & Levinstein, B. A. Standards for belief representations in LLMs. *Minds Mach.* **35**, 5. <https://doi.org/10.1007/s11023-024-09709-6> (2024).
25. Angelopoulos, A. N., Bates, S. *et al.* Confor-
mal prediction: A gentle introduction. *Founda-
tions Trends Mach. Learn.* **16**, 494–591. <https://doi.org/10.1561/2200000101> (2023).
26. Wikipedia contributors. List of fictional settle-
ments (2025). https://en.wikipedia.org/wiki/List_of_fictional_settlements.
27. Wikipedia contributors. List of fictional city-states in literature (2025). https://en.wikipedia.org/wiki/List_of_fictional_city-states_in_literature.
28. Fandom NeoEncyclopedia. List of fictional dis-
eases. https://neencyclopedia.fandom.com/wiki/List_of_fictional_diseases.
29. Fandom NeoEncyclopedia. List of fictional tox-
ins. https://neencyclopedia.fandom.com/wiki/List_of_fictional_toxins.
30. Chemeurope Encyclopedia. List of fictional med-
icines and drugs. https://www.chemeurope.com/en/encyclopedia>List_of_fictional_medicines_and_drugs.html.
31. Tomasula, S. The Thackery T. Lambshead pocket guide to eccentric & discredited diseases. *The Rev. Contemp. Fiction* **24** (2004).
32. Almaden, S. A. Dahl dictionary: A list of 103 words made-up by Roald Dahl (2023). <https://beelinguapp.com/blog/Dahl%20Dictionary:%20A%20List%20of%20103%20Words%20Made-up%20By%20Roald%20Dahl>.
33. Schleitwiler, P. & Shuflin, G. Dothraki initial text. <https://conlang.org/language-creation-conference/lcc5/1-dothraki-initial-text/>.
34. Dict-Na'vi.com Online Dictionary. wordlist “substan-
tive (noun)”. <https://dict-navi.com/en/dictionary/list/?type=classification&ID=1>.
35. Wolf, T. *et al.* Transformers: State-of-the-art natural language processing. In *Proceedings of the 2020 Conference on Empirical Methods in Natural Language Processing: System Demonstrations*, 38–45. <https://doi.org/10.18653/v1/2020.emnlp-demos.6> (2020).

A Notation

We summarize the mathematical notation used throughout the manuscript in Table A1.

Table A1. Notation. Summary of symbols used throughout the manuscript.

Symbol	Description
\mathcal{M}	A given LLM.
N	Number of statements in the dataset.
$\mathcal{S} = \{s_i\}_{i=1}^N$	Set of natural-language statements.
y_i	Ground-truth label of s_i : {True, False, Neither}.
l	Index of the LLM layer used for activation extraction.
$\mathbf{z}_i^{(l)}$	Activation vector for statement s_i at layer l .
$\mathcal{D} = \{(\mathbf{z}_i^{(l)}, y_i)\}_{i=1}^N$	Full activation-label dataset.
$\mathcal{D}_{\text{train}}, \mathcal{D}_{\text{cal}}, \mathcal{D}_{\text{test}}$	Train, calibration, and test splits of \mathcal{D} .
$y'_i \in \{+1, -1\}$	Baseline binary label: +1 for True, and -1 for False/Neither.
$f(\mathbf{z}) = \vec{w} \cdot \mathbf{z} + b$	Linear decision function of the baseline probe.
\vec{w}	Learned “truth direction” for the baseline probe.
b	Bias term of the baseline probe.
\hat{y}_i	Predicted label of the baseline probe for s_i .
$\mathcal{B}_{\text{true}} = \{s_i \mid \mathbf{z}_i^{(l)} \in \mathcal{D}_{\text{test}}, y_i = \text{True}, \hat{y}_i = +1\}$	True statements classified as true (baseline belief set).
\mathcal{N}	Set of all Neither statements.
$\mathcal{N}_1, \mathcal{N}_0$	Partition of \mathcal{N} : those re-labeled as True (\mathcal{N}_1) versus Not True (\mathcal{N}_0).
$y''_i \in \{+1, -1\}$	Perturbed binary label under a given $\mathcal{N}_1/\mathcal{N}_0$ split.
\vec{w}', b'	Truth direction and bias learned by the perturbed probe.
\hat{y}'_i	Predicted label of the perturbed probe.
$\mathcal{B}'_{\text{true}} = \{s_i \mid \mathbf{z}_i^{(l)} \in \mathcal{D}_{\text{test}}, y_i = \text{True}, \hat{y}'_i = +1\}$	True statements classified as true under the perturbed probe.

B Data

B.1 Data Generation

We use statements from the City Locations, Medical Indications, and Word Definitions datasets introduced in [12]. City statements take the form “*The city of [city] is (not) located in [country]*,” (omitting “*The city of*” when redundant). Medical statements follow “[drug] is (not) indicated for the treatment of [disease/condition].” Word Definition statements draw from three templates: “[word] is (not) a [instanceOf],” “[word] is (not) a type of [typeOf],” and “[word] is (not) a synonym of [synonym].”

B.1.1 True, False, and Synthetic Statements

We take the True, False, and Synthetic statements from the datasets introduced in [12]. All statements are constructed with both affirmative and negated forms. Synthetic entities are generated using a Markov-chain-based name generator (namemaker⁴) and undergo multi-stage filtering, including database checks, model tagging, and web-search validation, to ensure no accidental overlap with real entities. Validated names are then paired to form grammatically coherent but semantically meaningless statements that follow each template. Because Synthetic entities do not exist and cannot have appeared in training corpora, LLMs have no basis for assigning them a truth value. Accordingly, these statements function as Neither cases: unknown claims for which belief should be suspended rather than confidently classified as true or false.

B.1.2 Fictional Statements

In addition to Synthetic statements, which represent *unseen and unknown* claims, we construct new sets of Fictional statements for all three domains. Fictional statements also function as Neither statements in our experiments as they reference entities that do not exist in the real world and therefore lack real-world truth value. However, unlike Synthetic statements, many Fictional entities are likely to have appeared in LLM training corpora.⁵ As such, they represent a complementary form of Neither: claims that an LLM may recognize, but that still lie outside the true–false axis relevant to factual grounding.

⁴<https://github.com/Rickmsd/namemaker>

⁵For later analyses, we additionally annotate fictional statements with their within-universe factual status (Fictional True or Fictional False), but this labeling is not used in the primary True vs. Not True classification tasks.

To ensure that **Fictional** statements remain genuinely non-factual, all terms were validated to exclude any real-world overlap, and fictional lexical items appearing in any natural language were excluded to prevent misinterpretation by multilingual LLMs. **Fictional** statements were then constructed using the same templates as the **True**, **False**, and **Synthetic** statements, including both affirmative and negated forms.

Fictional City Locations. Fictional cities and countries are sourced from [26, 27], spanning literature, film, radio, television, comics, animation, and games. Each \langle city, location \rangle pair is included only when an identifiable enclosing region exists. When multiple spatial resolutions are available, we select the most specific (e.g., \langle Quahog, Rhode Island \rangle rather than \langle Quahog, United States \rangle).

Fictional Medical Indications. Fictional drug and disease statements are drawn from (1) *NeoEncyclopedia Wiki* [28, 29]; (2) ChemEurope’s *List of Fictional Medicines and Drugs* [30]; and (3) *The Thackery T. Lambshead Pocket Guide to Eccentric & Discredited Diseases* [31]. Drug–disease pairs are included when a treatment relationship exists within the fictional source.

Fictional Word Definitions. Fictional lexical items are compiled from (1) *Gobblefunk* [32]; (2) *Dothraki* [33]; and (3) *Na’vi* [34]. Dothraki and Na’vi have formal linguistic structure, whereas Gobblefunk is a playful neologistic extension of English.

B.1.3 Noise

The **Noise** statements contains no linguistic content. We generate $n_{\text{noise}} = 0.10 \cdot |\mathcal{D}|$ random activation sequences by sampling from a multivariate Gaussian with per-feature mean, standard deviation, and sequence-length distribution matched to the LLM activations. These distributionally consistent but non-semantic sequences serve as a control, allowing us to test whether observed representational differences arise from semantic content or from statistical variation in activation space.

B.2 Data Splits for Probing Experiments

Table A2. Dataset splits. The number of statements used in training, calibration, and testing of the probe. The proportion of total statements is reported in parentheses.

Dataset	Train	Calibration	Test	Total
City Locations	4746 (0.54)	1772 (0.20)	2229 (0.25)	8747 (1.00)
Medical Indications	4636 (0.55)	1721 (0.20)	2121 (0.25)	8478 (1.00)
Definitions	6488 (0.54)	2514 (0.21)	3041 (0.25)	12043 (1.00)

Table A2 summarizes the dataset partitions used for all probing experiments. Each dataset is split exclusively into training, calibration, and test sets to prevent data leakage. Approximately 55% of statements are used for training, 20% for calibration, and 25% for testing. We use identical splits across all probes and all LLMs, enabling direct comparison of representational stability under matched data conditions.

C LLMs

Table A3 lists the sixteen open-source LLMs used in our stability experiments. The set spans four major model families, Gemma, Llama, Mistral, and Qwen, with between about 3 billion to about 15 billion parameters and release dates between February and September 2024. For each family, we include both base (pre-trained) and chat-tuned variants to capture differences introduced by instruction fine-tuning. Together, these models provide a representative cross-section of current decoder-only architectures varying in scale, origin, and training objectives.

D Representations of True, False, and Neither by LLM

Supplementary Figures A1-A16 show the pairwise activation distance matrices for all sixteen LLMs. Three general representational patterns emerge. The first, observed in `_gemma-2-9b` (Fig. A1) and `gemma-2-9b` (Fig. A10), shows **Fictional** and **Synthetic** statements clustering near **True** and **False** statements, with **Noise** forming a distinct outlier. The second, present in `_gemma-7b` (Fig. A2), `gemma-7b` (Fig. A10), `_qwen-2.5-14b` (Fig. A8), `qwen-2.5-14b` (Fig. A15), and `_qwen-2.5-7b` (Fig. A9), exhibits **Synthetic** statements close to **True** and **False**, **Fictional** statements clearly separated, and **Noise** positioned slightly closer to the **True/False/Synthetic** cluster. The third, seen in the remaining nine models, features **Synthetic** statements aligned with **True** and **False**, while

Table A3. LLMs used in the stability experiments. We list the official names of the LLMs according to the HuggingFace repository [35]. We further specify the shortened name we use to refer to each of the models, whether it is the base, pre-trained model or a chat-tuned version, the number of decoders, the number of parameters, the release date, and the source of the model. Finally, we report the layers with the best separation between **True** and **Not True** statements for the City Locations (“C”), Medical Indications (“M”), and Word Definitions (“W”) datasets. The LLMs are publicly available through HuggingFace [35].

Official Name	Short Name	Type	# Decoders	# Parameters	Best Layer	Release Date	Source
Gemma-7b	gemma-7b	Base	28	8.54 B	C: 14, M: 19, W: 17	Feb 21, 2024	Google
Gemma-2-9b	gemma-2-9b	Base	26	9.24 B	C: 24, M: 25, W: 23	Jun 27, 2024	Google
Llama-3-8b	llama-3-8b	Base	32	8.03 B	C: 18, M: 17, W: 17	Jul 23, 2024	Meta
Llama-3.2-3b	llama-3.2-3b	Base	28	3.21 B	C: 16, M: 17, W: 15	Sep 25, 2024	Meta
Mistral-7B-v0.3	mistral-7B-v0.3	Base	32	7.25 B	C: 18, M: 17, W: 18	May 22, 2024	Mistral AI
Qwen2.5-7B	qwen-2.5-7b	Base	28	7.62 B	C: 18, M: 19, W: 17	Sep 19, 2024	Alibaba Cloud
Qwen2.5-14B	qwen-2.5-14b	Base	38	14.80 B	C: 30, M: 31, W: 30	Sep 19, 2024	Alibaba Cloud
Gemma-7b-it	_gemma-7b	Chat	28	8.54 B	C: 19, M: 19, W: 17	Feb 21, 2024	Google
Gemma-2-9b-it	_gemma-2-9b	Chat	26	9.24 B	C: 27, M: 26, W: 25	Jul 27, 2024	Google
Llama-3.2-3b-Instruct	_llama-3.2-3b	Chat	28	3.21 B	C: 16, M: 19, W: 18	Sep 25, 2024	Meta
Llama-3.1-8b-Instruct	_llama-3.1-8b	Chat	32	8.03 B	C: 18, M: 19, W: 18	Jul 23, 2024	Meta
Llama3-Med42-8b	_llama-3-8b-med	Chat	32	8.03 B	C: 18, M: 16, W: 15	Aug 12, 2024	M42 Health
Bio-Medical-Llama-3-8b	_llama-3-8b-bio	Chat	32	8.03 B	C: 18, M: 19, W: 18	Aug 11, 2024	Contact Doctor
Mistral-7b-Instruct-v0.3	_mistral-7B-v0.3	Chat	32	7.25 B	C: 19, M: 21, W: 18	May 22, 2024	Mistral AI
Qwen2.5-7B-Instruct	_qwen-2.5-7b	Chat	28	7.62 B	C: 19, M: 21, W: 18	Aug 18, 2024	Alibaba Cloud
Qwen2.5-14B-Instruct	_qwen-2.5-14b	Chat	38	14.80 B	C: 31, M: 34, W: 30	Aug 18, 2024	Alibaba Cloud

_gemma-2-9b: Wasserstein Distance between Activations

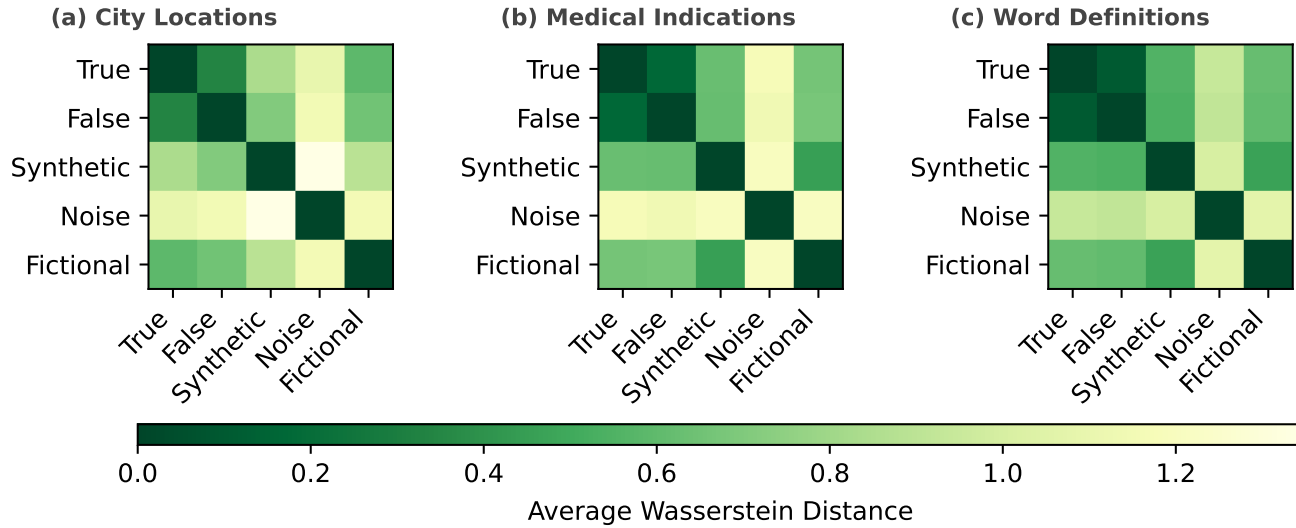


Figure A1. Wasserstein distance between activations for `_gemma-2-9b`. Pairwise Wasserstein distances between activation distributions of **True**, **False**, **Synthetic**, **Fictional**, and **Noise** statements for the (a) City Locations, (b) Medical Indications, and (c) Word Definitions datasets. **Noise** has distinct representations, but **Fictional** and **Synthetic** statements are represented similarly to **True** and **False** statements and each other.

both **Fictional** and **Noise** statements occupy distinct and distant regions. Except for **qwen-2.5-7b** (which follows the second pattern; Fig. A9) and **qwen-2.5-7b** (the third; Fig. A16), base and chat versions of each model display qualitatively similar representational structures.

gemma-7b: Wasserstein Distance between Activations

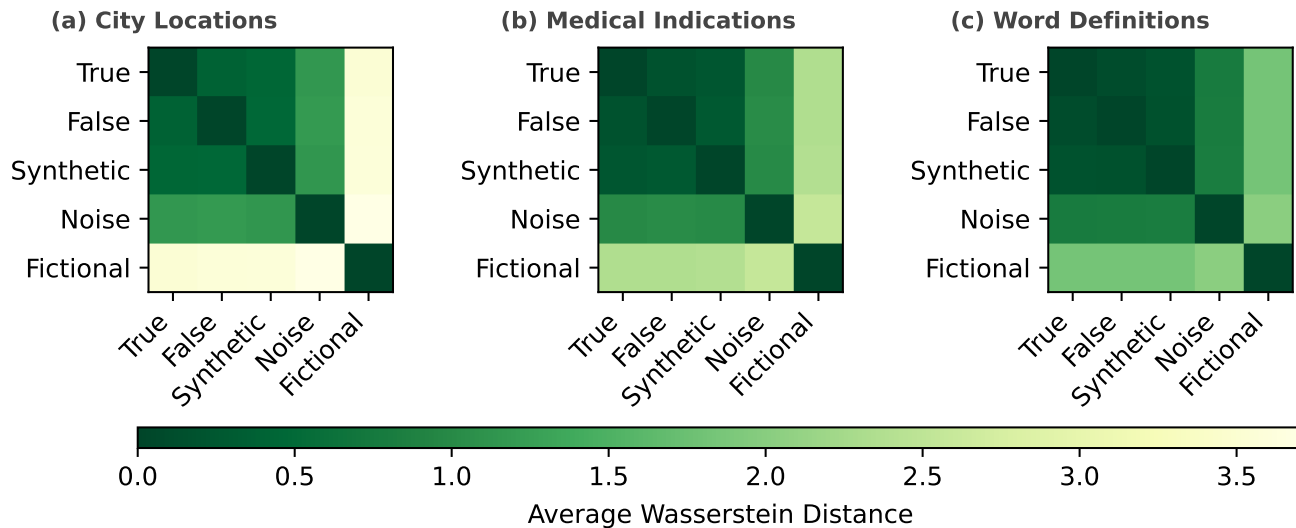


Figure A2. Wasserstein distance between activations for `gemma-7b`. Pairwise Wasserstein distances between activation distributions of True, False, Synthetic, Fictional, and Noise statements for the (a) City Locations, (b) Medical Indications, and (c) Word Definitions datasets. Synthetic statements are represented similarly to True and False statements, while Fictional statements are represented distinctly from all other statements.

llama-3-8b-med: Wasserstein Distance between Activations

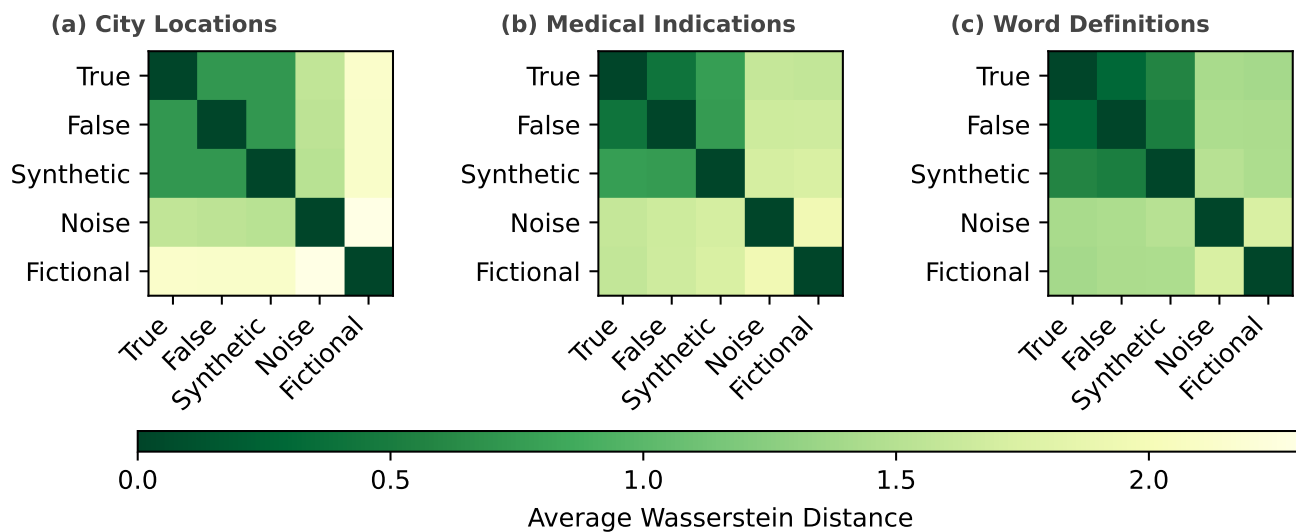


Figure A3. Wasserstein distance between activations for `llama-3-8b-med`. Pairwise Wasserstein distances between activation distributions of True, False, Synthetic, Fictional, and Noise statements for the (a) City Locations, (b) Medical Indications, and (c) Word Definitions datasets. Synthetic statements are represented similarly to True and False statements, while Fictional statements and Noise are represented distinctly from all other statements.

_llama-3.1-8b-bio: Wasserstein Distance between Activations

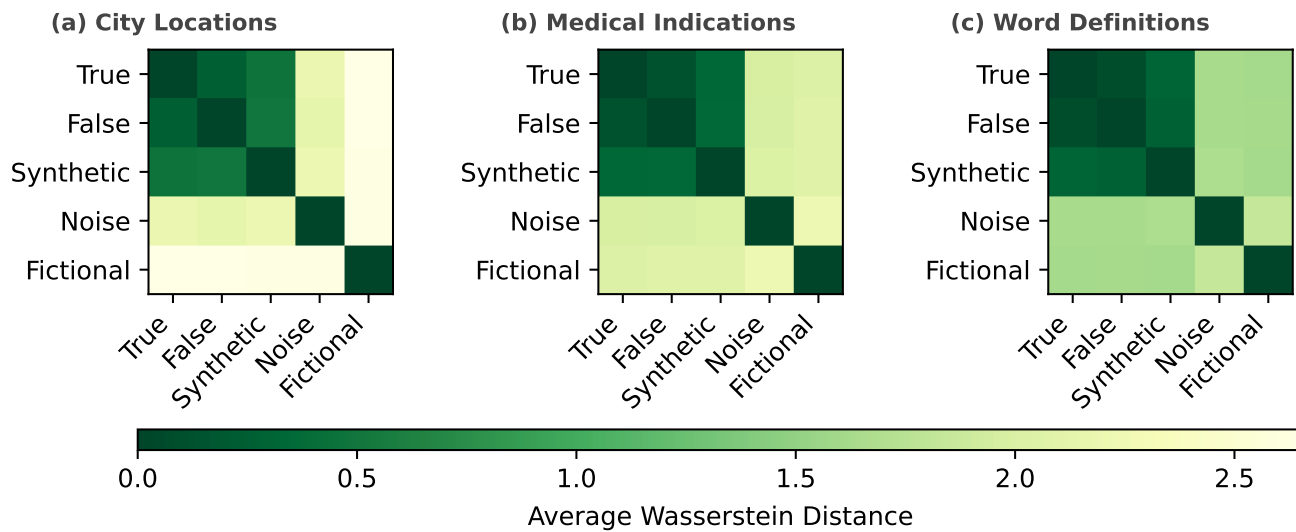


Figure A4. Wasserstein distance between activations for `_llama-3-8b-bio`. Pairwise Wasserstein distances between activation distributions of True, False, Synthetic, Fictional, and Noise statements for the (a) City Locations, (b) Medical Indications, and (c) Word Definitions datasets. Synthetic statements are represented similarly to True and False statements, while Fictional statements and Noise are represented distinctly from all other statements.

_llama-3.1-8b: Wasserstein Distance between Activations

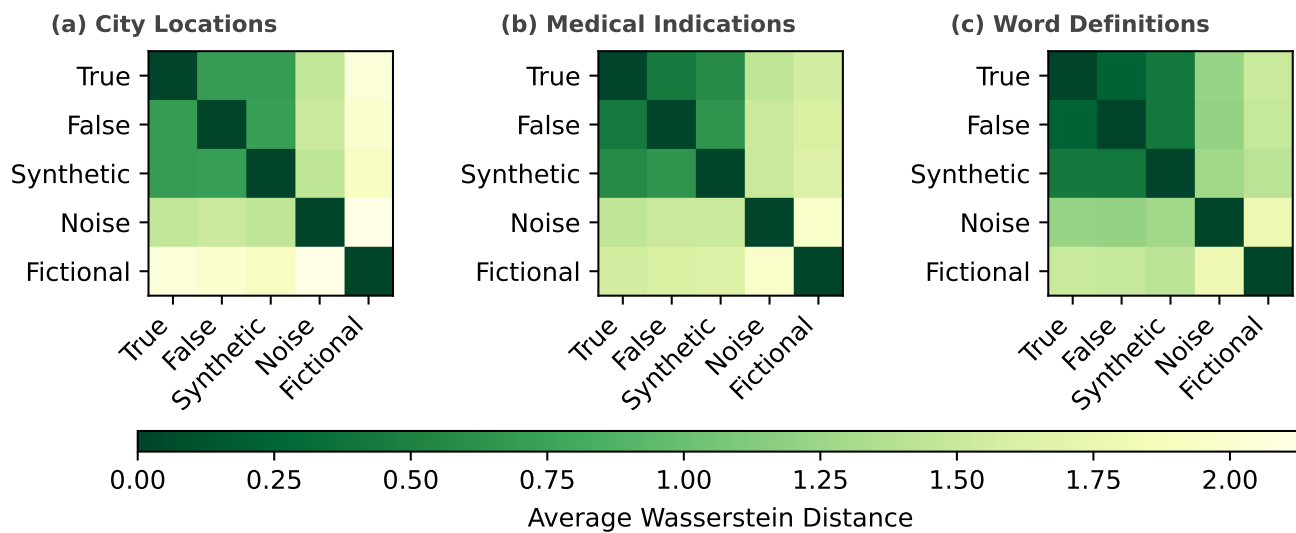


Figure A5. Wasserstein distance between activations for `_llama-3.1-8b`. Pairwise Wasserstein distances between activation distributions of True, False, Synthetic, Fictional, and Noise statements for the (a) City Locations, (b) Medical Indications, and (c) Word Definitions datasets. Synthetic statements are represented similarly to True and False statements, while Fictional statements and Noise are represented distinctly from all other statements.

_llama-3.2-3b: Wasserstein Distance between Activations

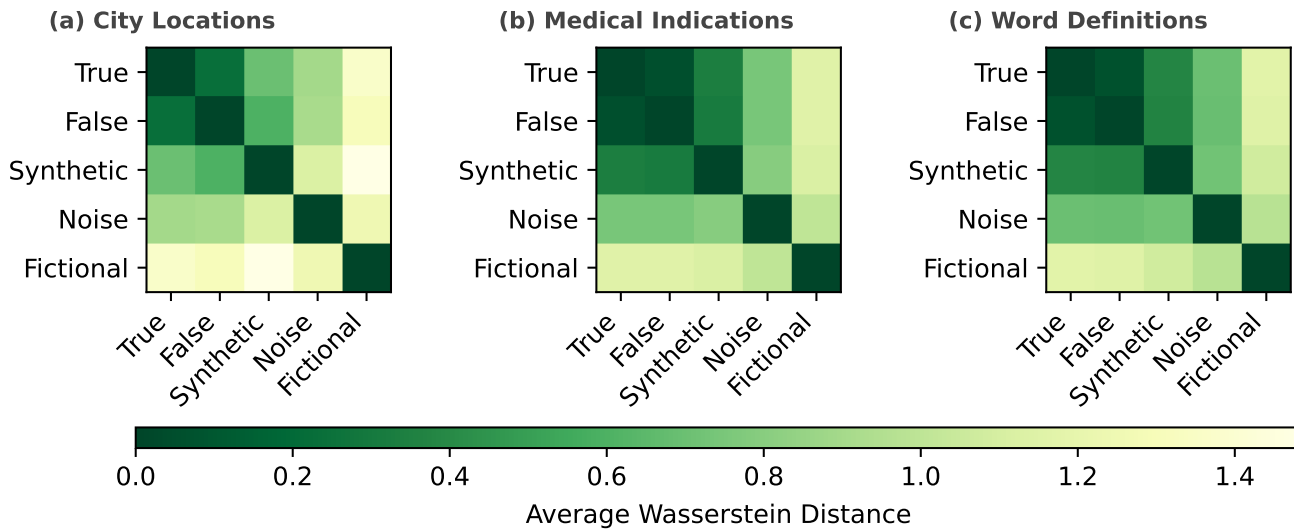


Figure A6. Wasserstein distance between activations for `_llama-3.2-3b`. Pairwise Wasserstein distances between activation distributions of True, False, Synthetic, Fictional, and Noise statements for the (a) City Locations, (b) Medical Indications, and (c) Word Definitions datasets. Synthetic statements are represented similarly to True and False statements, while Fictional statements and Noise are represented distinctly from all other statements.

_mistral-7B-v0.3: Wasserstein Distance between Activations

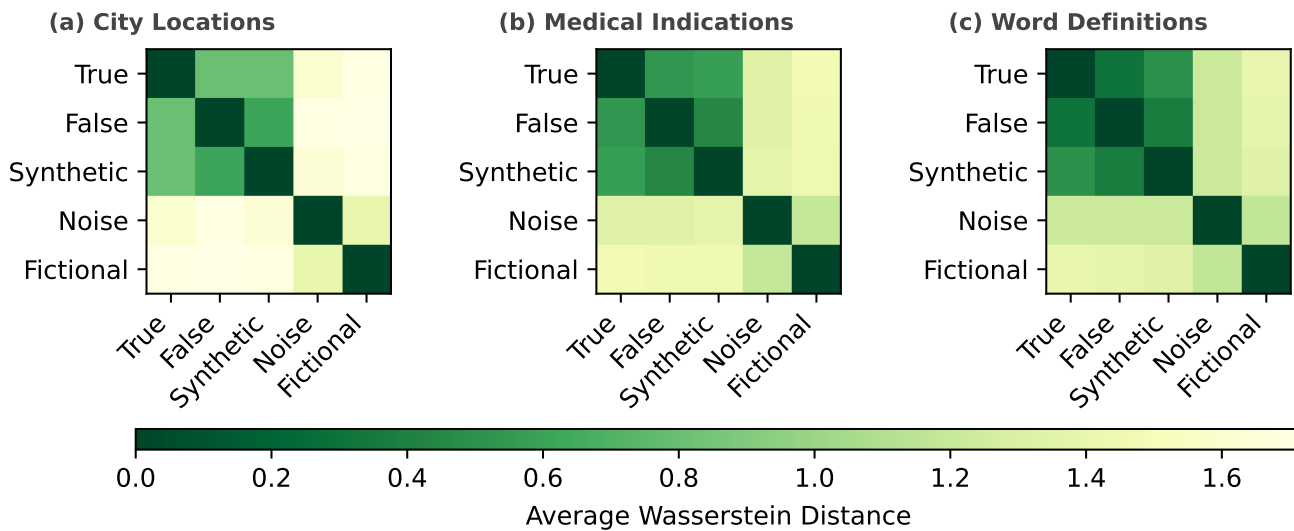


Figure A7. Wasserstein distance between activations for `_mistral-7B-v0.3`. Pairwise Wasserstein distances between activation distributions of True, False, Synthetic, Fictional, and Noise statements for the (a) City Locations, (b) Medical Indications, and (c) Word Definitions datasets. Synthetic statements are represented similarly to True and False statements, while Fictional statements and Noise are represented distinctly from all other statements.

_qwen-2.5-14b: Wasserstein Distance between Activations

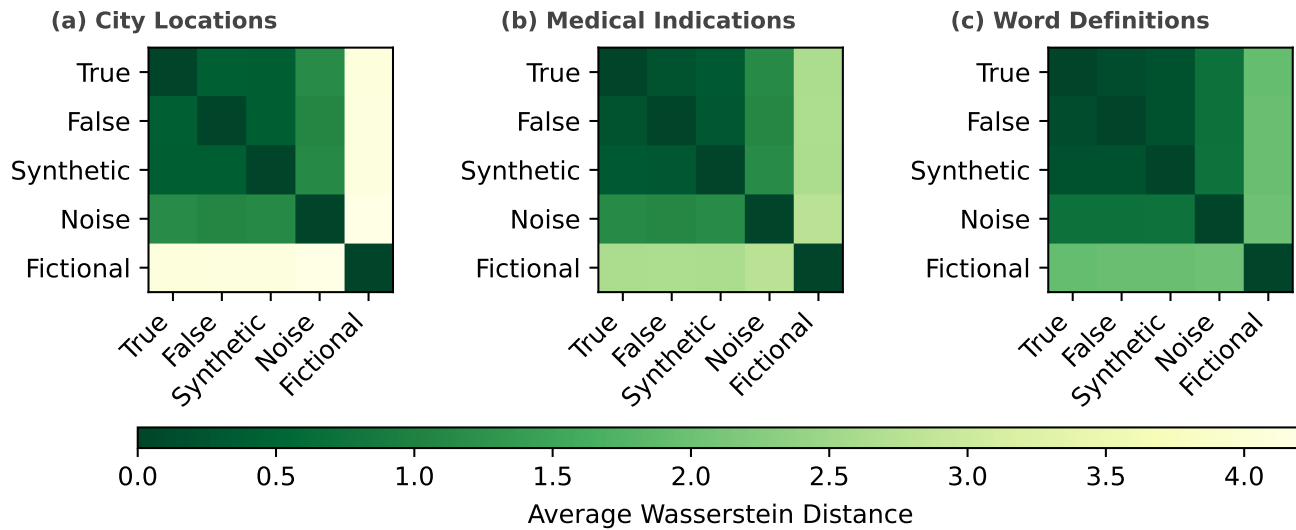


Figure A8. Wasserstein distance between activations for `_qwen-2.5-14b`. Pairwise Wasserstein distances between activation distributions of True, False, Synthetic, Fictional, and Noise statements for the (a) City Locations, (b) Medical Indications, and (c) Word Definitions datasets. Synthetic statements are represented similarly to True and False statements, while Fictional statements are represented distinctly from all other statements.

_qwen-2.5-7b: Wasserstein Distance between Activations

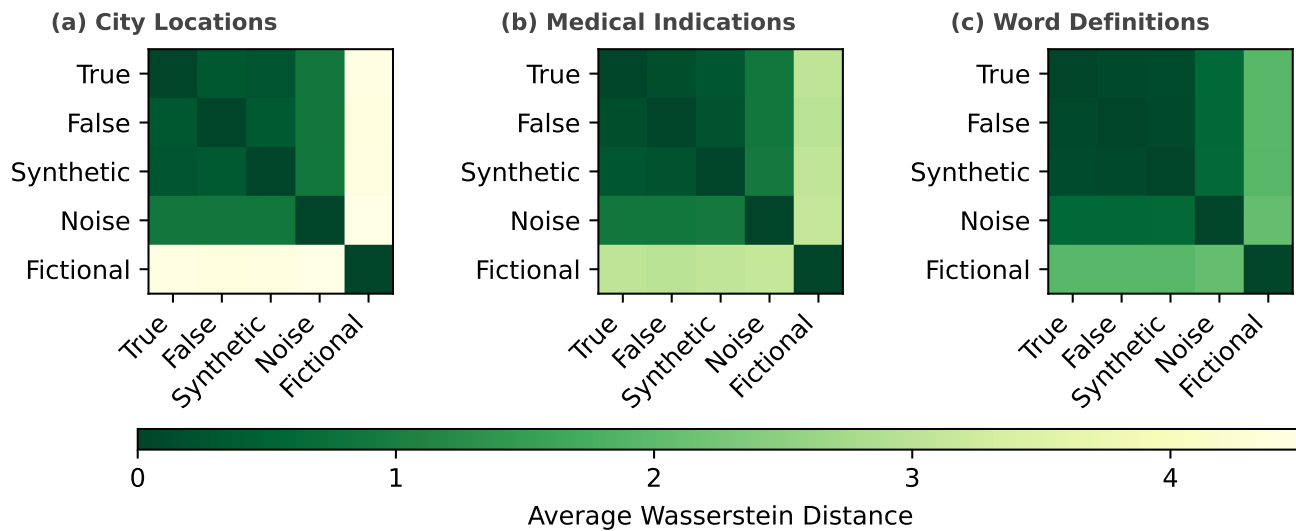


Figure A9. Wasserstein distance between activations for `_qwen-2.5-7b`. Pairwise Wasserstein distances between activation distributions of True, False, Synthetic, Fictional, and Noise statements for the (a) City Locations, (b) Medical Indications, and (c) Word Definitions datasets. Synthetic statements are represented similarly to True and False statements, while Fictional statements are represented distinctly from all other statements.

gemma-2-9b: Wasserstein Distance between Activations

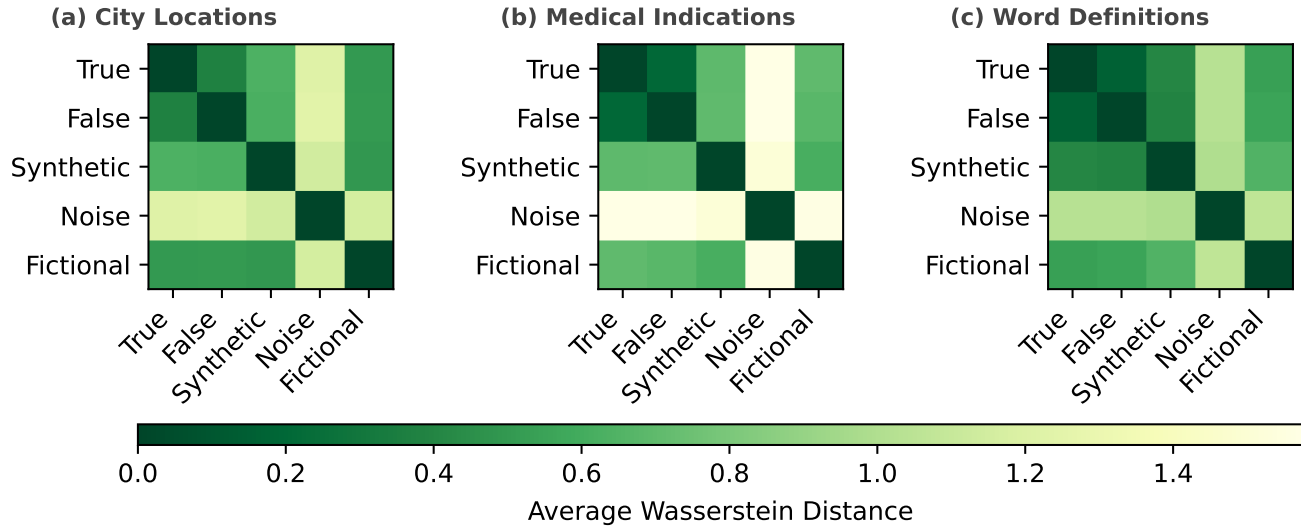


Figure A10. Wasserstein distance between activations for gemma-2-9b. Pairwise Wasserstein distances between activation distributions of True, False, Synthetic, Fictional, and Noise statements for the (a) City Locations, (b) Medical Indications, and (c) Word Definitions datasets. Noise has distinct representations, but Fictional and Synthetic statements are represented similarly to True and False statements and each other.

gemma-7b: Wasserstein Distance between Activations

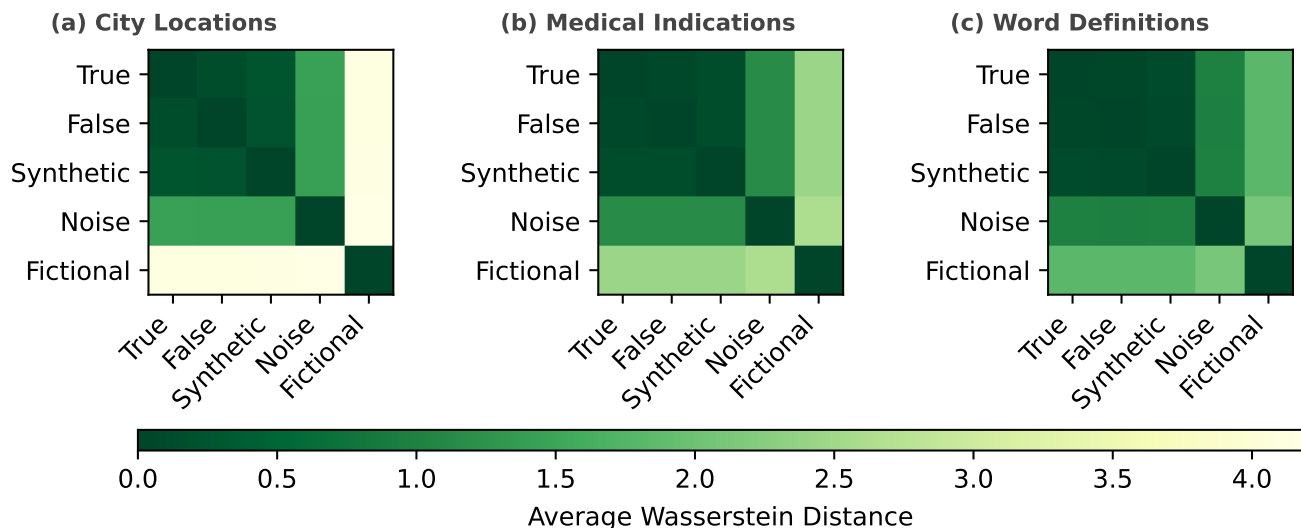


Figure A11. Wasserstein distance between activations for gemma-7b. Pairwise Wasserstein distances between activation distributions of True, False, Synthetic, Fictional, and Noise statements for the (a) City Locations, (b) Medical Indications, and (c) Word Definitions datasets. Synthetic statements are represented similarly to True and False statements, while Fictional statements are represented distinctly from all other statements.

llama-3-8b: Wasserstein Distance between Activations

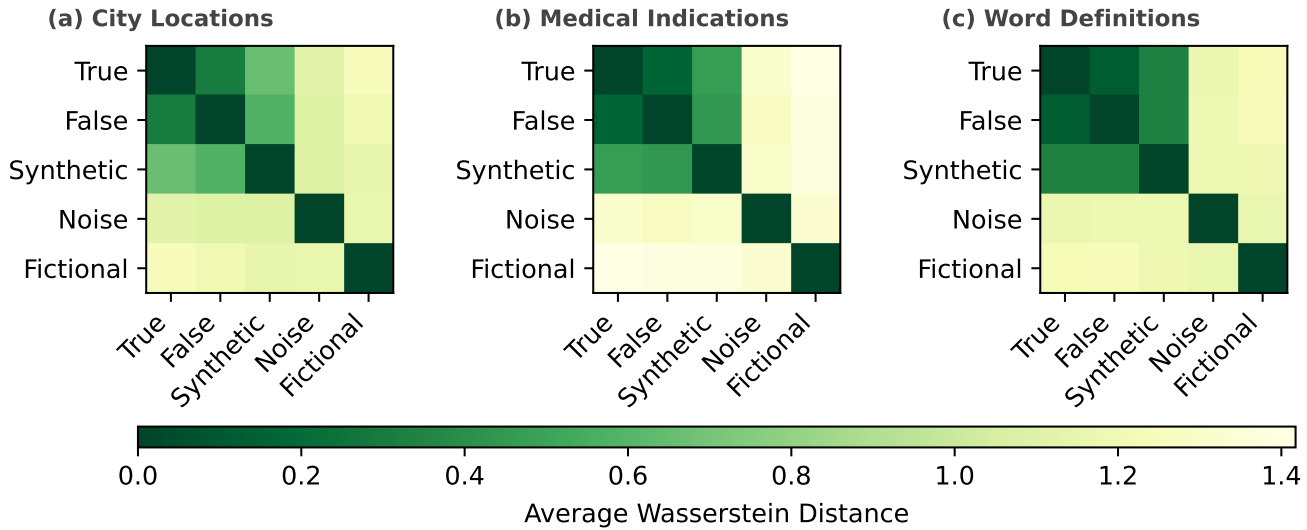


Figure A12. Wasserstein distance between activations for llama-3-8b. Pairwise Wasserstein distances between activation distributions of True, False, Synthetic, Fictional, and Noise statements for the (a) City Locations, (b) Medical Indications, and (c) Word Definitions datasets. Synthetic statements are represented similarly to True and False statements, while Fictional statements and Noise are represented distinctly from all other statements.

llama-3.2-3b: Wasserstein Distance between Activations

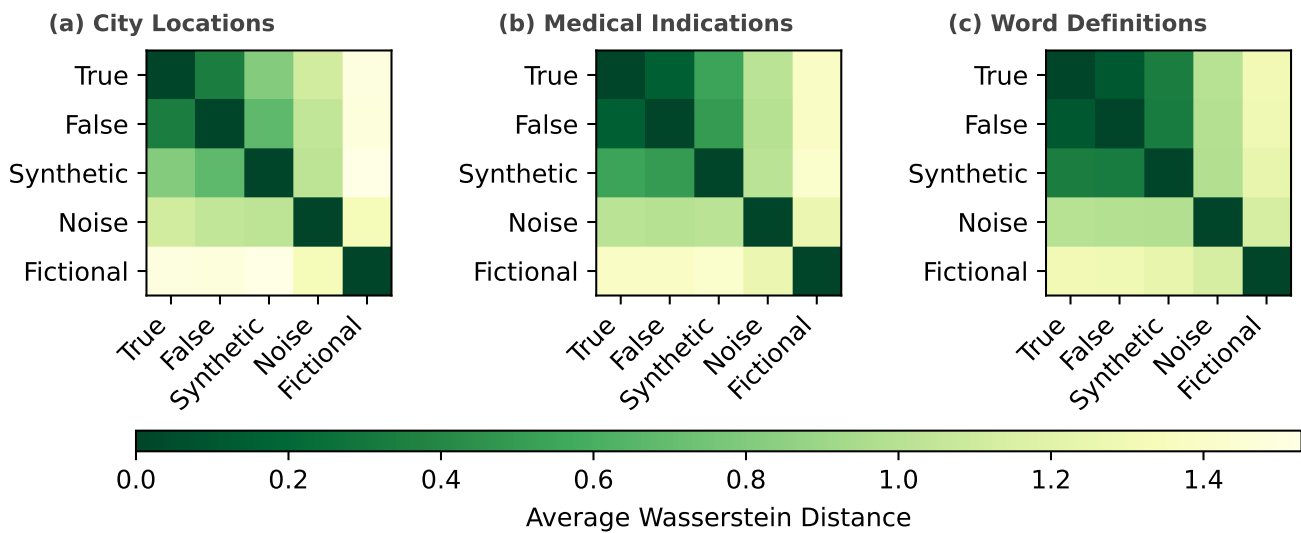


Figure A13. Wasserstein distance between activations for llama-3.2-3b. Pairwise Wasserstein distances between activation distributions of True, False, Synthetic, Fictional, and Noise statements for the (a) City Locations, (b) Medical Indications, and (c) Word Definitions datasets. Synthetic statements are represented similarly to True and False statements, while Fictional statements and Noise are represented distinctly from all other statements.

mistral-7B-v0.3: Wasserstein Distance between Activations

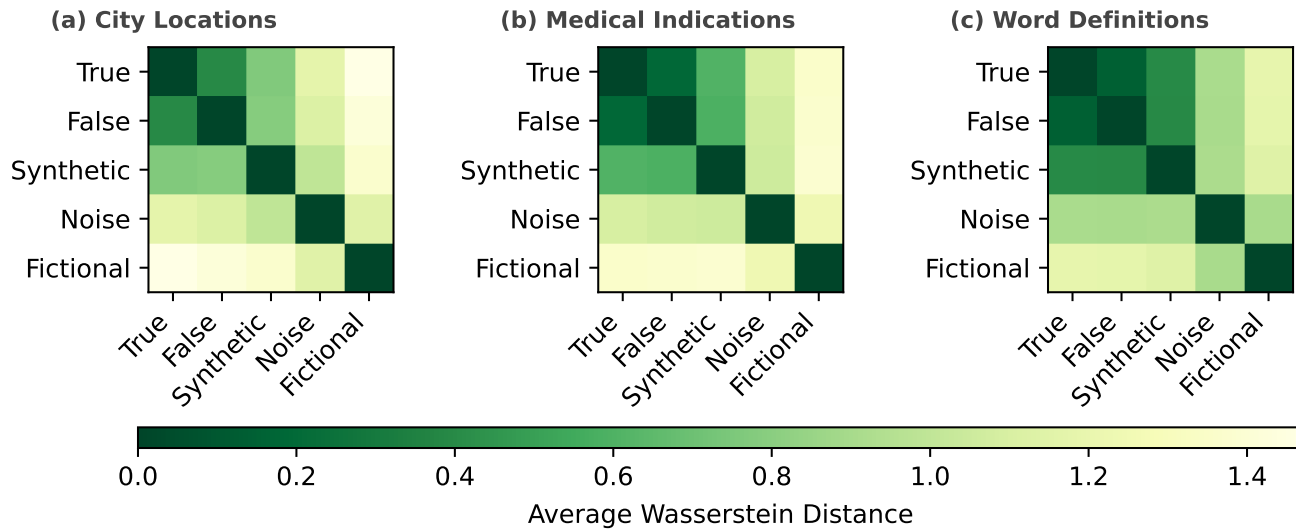


Figure A14. Wasserstein distance between activations for `mistral-7B-v0.3`. Pairwise Wasserstein distances between activation distributions of True, False, Synthetic, Fictional, and Noise statements for the (a) City Locations, (b) Medical Indications, and (c) Word Definitions datasets. Synthetic statements are represented similarly to True and False statements, while Fictional statements and Noise are represented distinctly from all other statements.

qwen-2.5-14b: Wasserstein Distance between Activations

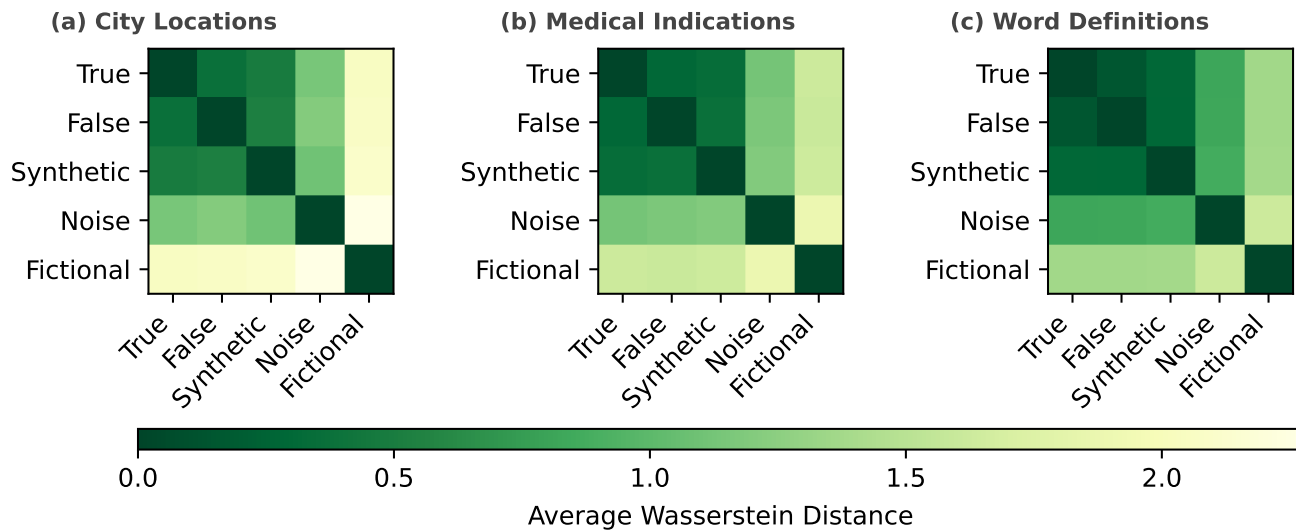


Figure A15. Wasserstein distance between activations for `qwen-2.5-14b`. Pairwise Wasserstein distances between activation distributions of True, False, Synthetic, Fictional, and Noise statements for the (a) City Locations, (b) Medical Indications, and (c) Word Definitions datasets. Synthetic statements are represented similarly to True and False statements, while Fictional statements are represented distinctly from all other statements.

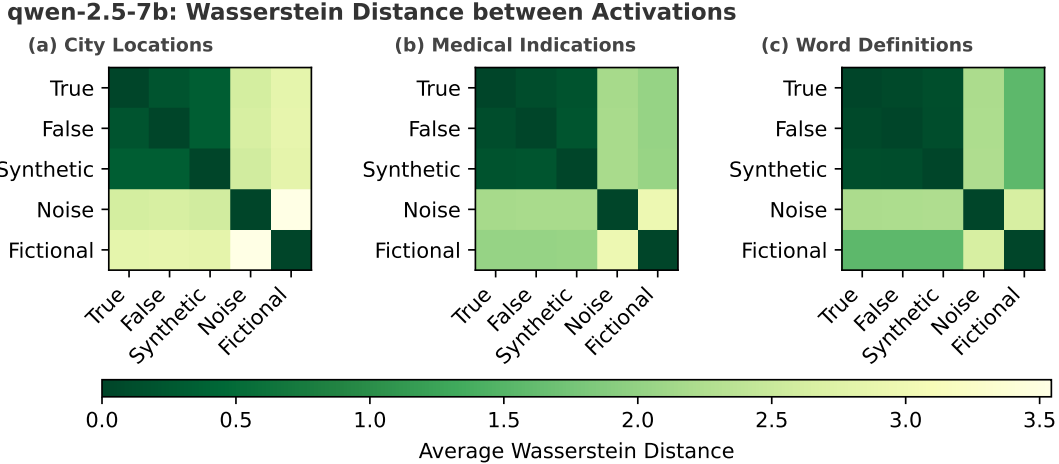


Figure A16. Wasserstein distance between activations for qwen-2.5-7b. Pairwise Wasserstein distances between activation distributions of True, False, Synthetic, Fictional, and Noise statements for the (a) City Locations, (b) Medical Indications, and (c) Word Definitions datasets. Synthetic statements are represented similarly to True and False statements, while Fictional statements and Noise are represented distinctly from all other statements.

E Exploring Additional Probes

We repeated the label perturbation experiments using the **Mean Difference** probe proposed by Marks and Tegmark [13]. It estimates a “truth direction” by taking the vector difference between the mean activation of **True** statements and that of **False** statements, optionally scaled by the inverse covariance matrix of the data. This approach is inherently sensitive to differences in the centroids and covariance structure of the data, which leads to strong instability in the learned decision boundary when **Neither** statements are included alongside true and false examples. The **Mean Difference** probe shows considerably greater variability across LLMs than **sAwMIL** (Fig. A17). While **sAwMIL** yields consistent decision boundary rotation corresponding to specific perturbations, particularly the **Synthetic** perturbation, the **Mean Difference** probe exhibits near-orthogonal boundary shifts for certain LLMs regardless of perturbation. In addition, Table A4 shows that, unlike with **sAwMIL**, the **Fictional** perturbation produces the largest number of prediction flips across all three datasets, and the Word Definitions dataset exhibits the fewest total flips. We interpret these discrepancies as artifacts of the **Mean Difference** probe’s reliance on dataset centroids: when statement activations are well separated, as with **Fictional** statements, class-label perturbations can induce disproportionately large changes in the estimated decision boundary. This instability reflects probe sensitivity rather than genuine representational instability in the LLMs. Accordingly, the **Mean Difference** probe is less well suited for quantifying representational stability than **sAwMIL**.

Table A4. Flipped predictions under label perturbations for the Mean Difference Probe. Counts (and percentages) of predictions that remain stable or flip between True and Not True across Synthetic, Fictional, Fictional(T), and Noise perturbations for each dataset. Word Definitions is the most stable, followed by City Locations and Medical Definitions. The Fictional perturbation leads to the most instability.

Dataset	Perturbation	True to True	Not True to Not True	Not True to True	True to Not True	Total Flips
City Locations	Synthetic	9724 (97.2)	167 (1.7)	63 (0.6)	46 (0.5)	109 (1.1)
	Fictional	7386 (73.9)	221 (2.2)	9 (0.1)	2384 (23.8)	2393 (23.9)
	Fictional (T)	9680 (96.8)	184 (1.8)	46 (0.5)	90 (0.9)	136 (1.4)
	Noise	9653 (96.5)	201 (2.0)	29 (0.3)	117 (1.2)	146 (1.5)
Medical Locations	Synthetic	9457 (86.8)	894 (8.2)	221 (2.0)	324 (3.0)	545 (5.0)
	Fictional	4694 (43.1)	977 (9.0)	138 (1.3)	5087 (46.7)	5225 (48.0)
	Fictional (T)	9718 (89.2)	1069 (9.8)	46 (0.4)	63 (0.6)	109 (1.0)
	Noise	8955 (82.1)	1026 (9.4)	89 (0.8)	826 (7.6)	915 (8.4)
Word Definitions	Synthetic	8468 (85.6)	500 (5.1)	695 (7.0)	225 (2.3)	920 (9.3)
	Fictional	7035 (71.1)	1175 (11.9)	20 (0.2)	1658 (16.8)	1678 (17.0)
	Fictional (T)	8282 (83.8)	1083 (11.0)	112 (1.1)	411 (4.2)	523 (5.3)
	Noise	8208 (83.0)	1178 (11.9)	17 (0.2)	485 (4.9)	502 (5.1)

Change in Mean Difference Decision Boundary under Perturbations

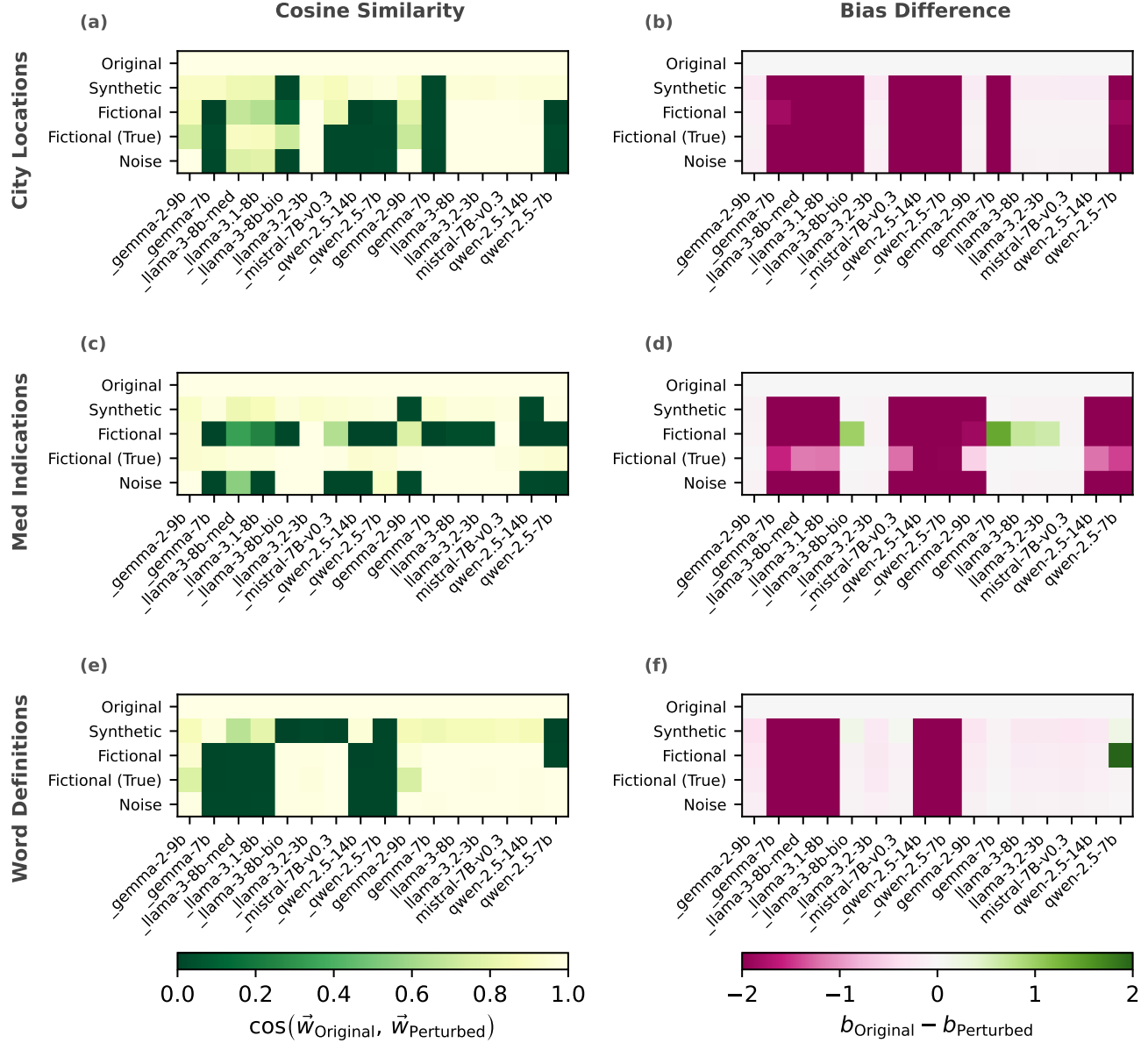


Figure A17. Change in Mean Difference decision boundaries under perturbations. Cosine similarity (left column) and bias difference (right column) between the baseline True vs. Not True probe and probes retrained under label perturbations for the (a,b) City Locations, (c,d) Medical Indications, and (e,f) Word Definitions datasets. Each heatmap shows results for sixteen LLMs (columns) and five perturbation conditions (rows). LLMs with leading underscores are chat models, while those without are base models. Higher cosine similarity indicates smaller rotations of the learned decision boundary, while bias difference reflects shifts in intercept. Certain LLMs lead to near orthogonal perturbed decision boundaries across all perturbation types, suggesting that, unlike sAwMIL, the probe is highly sensitive to differences in the distributions of the underlying activations.